CZECH TECHNICAL UNIVERSITY IN PRAGUE

FACULTY OF BIOMEDICAL ENGINEERING

Department of Biomedical Technology

Heating of Tumor Resection Cavities in Brain

Ohřev mozkové tkáně po resekci nádoru

Bachelor Thesis

Study program: Biomedical and Clinical Technology
Study branch: Biomedical Technician

Bachelor thesis supervisor: Doc. Ing. David Vrba, Ph.D.

Gabriela Liptáková

Kladno 2020

CTU
CZECH TECHNICAL UNIVERSITY IN PRAGUE

BACHELOR'S THESIS ASSIGNMENT

I. PERSONAL AND STUDY DETAILS

Student's name:	**Liptáková Gabriela**	Personal ID number: **465434**
Faculty:	**Faculty of Biomedical Engineering**	
Department:	**Department of Biomedical Technology**	
Study program:	**Biomedical and Clinical Technology**	
Branch of study:	**Biomedical Technician**	

II. BACHELOR'S THESIS DETAILS

Bachelor's thesis title in English:

Heating of Tumor Resection Cavities in Brain

Bachelor's thesis title in Czech:

Ohřev mozkové tkáně po resekci nádoru

Guidelines:

In Sim4Life platform create two numerical models. Import real dielectric model of patient´s head to the first one and a detailed model of head and neck "MIDA" from IT´IS Foundation to the second one. For both of these models create a resection cavity simulating surgical removal of brain tumor. Fill this cavity with a hot water ballon in the temperature range from 40 °C to 50 °C. Subsequently in the Sim4Life implement temperature dependence of brain tissue perfusion. Using a numerical simulation of heat transfer in biological tissues, calculate the heat distribution in the vicinity of the balloon. Perform the simulation for three different positions and sizes of the resection cavity. Evaluate the heating depth of brain tissue according to the location and size of the resection cavity. Compare the results from both numerical models.

Bibliography / sources:

[1] Vrba J.: Lékařské aplikace mikrovlnné techniky, ed. 1st, ČVUT Praha, 2003, ISBN 80-01-02705-8 (in Czech)

Name of bachelor's thesis supervisor:

doc. Ing. David Vrba, Ph.D.

Name of bachelor's thesis consultant:

doc. Dr.-Ing. Jan Vrba, M.Sc., MUDr. Luca Vannucci, Ph.D.

Date of bachelor's thesis assignment: **17.02.2020**
Assignment valid until: **19.09.2021**

Peter Kneppo Digitálně podepsal Peter Kneppo Datum: 2020.04.20 15:07:52 +02'00'

prof. Ing. Peter Kneppo, DrSc., dr.h.c.
Head of department's signature

prof. MUDr. Ivan Dylevský, DrSc. Digitálně podepsal prof. MUDr. Ivan Dylevský, DrSc. Datum: 2020.04.23 11:33:34 +02'00'

prof. MUDr. Ivan Dylevský, DrSc.
Dean's signature

ČVUT
ČESKÉ VYSOKÉ UČENÍ TECHNICKÉ V PRAZE

ZADÁNÍ BAKALÁŘSKÉ PRÁCE

I. OSOBNÍ A STUDIJNÍ ÚDAJE

Příjmení:	**Liptáková**	Jméno:	**Gabriela**	Osobní číslo:	**465434**
Fakulta:	**Fakulta biomedicínského inženýrství**				
Garantující katedra:	**Katedra biomedicínské techniky**				
Studijní program:	**Biomedicínská a klinická technika**				
Studijní obor:	**Biomedicínský technik**				

II. ÚDAJE K BAKALÁŘSKÉ PRÁCI

Název bakalářské práce:

Ohřev mozkové tkáně po resekci nádoru

Název bakalářské práce anglicky:

Heating of Tumor Resection Cavities in Brain

Pokyny pro vypracování:

V prostředí Sim4Life vytvořte dva numerické modely. Do prvního z nich importujte reálný dielektrický model hlavy pacienta a do druhého detailní model hlavy a krku MIDA od společnosti IT'IS Foundation. Pro oba modely vytvořte v modelu mozku dutinu simulující chirurgické odstranění nádoru (resekční dutinu). Tuto dutinu virtuálně vyplňte balónkem s teplou vodou o teplotě v rozsahu 40 - 50 °C. Do prostředí Sim4Life dále implementujte teplotní závislost perfuze mozkové tkáně. Pomocí numerické simulace šíření tepla v biologických tkáních vypočítejte rozložení teploty v okolí balónku. Tuto simulaci proveďte pro tři různé polohy a tři různé velikosti resekční dutiny. Vyhodnoťte hloubku prohřátí mozkové tkáně v závislosti na místě a velikosti resekční dutiny. Výsledky získané pomocí obou numerických modelů vzájemně porovnejte.

Seznam doporučené literatury:

[1] J. Vrba, Lékařské aplikace mikrovlnné techniky, ed. 1st, ČVUT Praha, 2003, ISBN 80-01-02705-8

Jméno a příjmení vedoucí(ho) bakalářské práce:

doc. Ing. David Vrba, Ph.D.

Jméno a příjmení konzultanta(ky) bakalářské práce:

doc. Dr.-Ing. Jan Vrba, MSc., MUDr. Luca Vannucci, Ph.D.

Datum zadání bakalářské práce: **17.02.2020**
Platnost zadání bakalářské práce: **20.09.2020**

Peter Kneppo Digitálně podepsal Peter Kneppo Datum: 2020.04.20 15:06:55 +02'00'

prof. Ing. Peter Kneppo, DrSc., dr.h.c.
podpis vedoucí(ho) katedry

prof. MUDr. Ivan Dylevský, DrSc. Digitálně podepsal prof. MUDr. Ivan Dylevský, DrSc. Datum: 2020.04.23 11:32:44 +02'00'

prof. MUDr. Ivan Dylevský, DrSc.
podpis děkana(ky)

DECLARATION

I hereby declare that I have completed this thesis having the topic “Heating of Tumor Resection Cavities in Brain” independently, and that I have attached an exhaustive list of citations of the used sources.

I do not have a compelling reason against the use of the thesis within the meaning of Section 60 of the Act No.121 / 2000 Sb., on copyright, rights related to copyright and amending some laws (the Copyright Act).

In Kladno 21st May 2020 Gabriela Liptáková

ACKNOWLEDGEMENTS

I would like to thank my supervisor, Doc. Ing. David Vrba, Ph.D. for his advice on the structure of this thesis, his patience and prompt responding to my questions about the topic of the thesis.

ABSTRACT

Heating of Tumor Resection Cavities in Brain

This thesis proposes one of the possible treatment methods for glioblastoma residues of possible metastatic nature after the resection of primary tumour. To avoid the aggressive spreading of cancer and potential formation of secondary tumours, the post-surgical treatment is proposed, combining brachytherapy, effectiveness of which is enforced by hyperthermia. The aim of the thesis is to find out how much can the tissue, surrounding resection cavity, be heated and therefore, how much can the radiation dose be reduced. The extent of heating is computed using Sim4Life platform on two cranial models differing in number of allowed tissues. For the coupling of brachytherapy and hyperthermia effects, a thermobrachytherapy balloon with nanoparticle solution is used, located in three most common locations of glioblastomas' incidence. For more accurate calculations, considering the hyperthermic conditions, the perfusion rates of chosen tissues were adjusted in accordance with the carried-out research. The results of these simulations were compared and analysed according to the option of heating method, choice of cranial model and the impact of hyperperfusion.

Key words

brachytherapy, hyperthermia, glioblastoma multiforme, perfusion

ABSTRAKT

Ohřev mozkové tkáně po resekci nádoru

Tato práce nabízí jednu z možných terapií zbytků glioblastomu s možným metastatickým charakterem po vyjmutí primárního nádoru. Abychom zabránili agresivnímu šíření nádorů a potenciálnímu tvoření sekundárních tumorů, nabízí se pooperační léčba, kombinující brachyterapii s účinky podpořenými hypertermií. Cílem práce je zjistit, jak intenzivně je možné tkáň kolem resekční dutiny zahřát, a tím případně snížit potřebnou radiační dávku. Míra zahřátí tkáně je počítána pomocí programu Sim4Life na dvou modelech hlavy, lišících se počtem zohledněných tkání. Pro sloučení účinků brachyterapie a hypertermie je použit termobrachyterapický balónek s roztokem nanočástic, umístěný ve třech nejčastějších místech výskytu glioblastomů. Pro přesnější výpočet, zohledňující hypertermické podmínky, byly upraveny hodnoty perfuze vybraných tkání na základě vykonané rešerše. Výsledky simulací byly porovnány a byl zhodnocen výběr metody zahřívání nanočásticemi, výběr modelu hlavy a vliv hyperperfuze.

Klíčova slova

brachyterapie, hypertermie, multiformní glioblastom, perfuze

Table of Contents

List of symbols and abbreviations

List of symbols

Symbol	Unit	Importance
G	$W \cdot kg^{-1}$	Heat generation rate
P	W	Power Loss
ρ	$kg \cdot m^3$	Mass density
m	kg	Mass
V	m^3	Volume
π	-	Pi, Archimedes' constant
r	m	Radius of the balloon
r_o	m	Radius of the outer balloon
r_i	m	Radius of the inner balloon
t	s	Time
T	K, °C	Temperature
$T_{outside}$	K, °C	Temperature of the environment
σ	$W \cdot m^{-2} \cdot K^{-4}$	Stefan-Boltzmann constant
h	$W \cdot m^{-2} \cdot K^{-1}$	Heat transfer coefficient
n	m	Thickness of a wall
C_p	$J \cdot kg^{-1} \cdot K^{-1}$	Specific Heat Capacity
λ	$W \cdot m^{-1} \cdot K^{-1}$	Thermal conductivity
∇	-	Nabla, differential operator
Q_{bio}	J	Heat of blood perfusion
Q_{met}	J	Metabolic heat
T_a	K, °C	Temperature of blood in arteries

List of abbreviations

Abbreviation	Importance
GBM	Glioblastoma Multiforme
TBT	Thermobrachytherapy
CBF	Cerebral blood flow
CNS	Central Nervous System
WHO	World Health Organisation
CT	Computed Tomography
MRI	Magnetic Resonance Imaging
SPECT	Single Photon Emission Computed Tomography
PET	Positron Emission Tomography
RT	Radiotherapy
TMZ	Temozolomide
LDR	Low Dose Rate
HDR	High Dose Rate
FDA	Food and Drug Administration
HGR	Heat Generation Rate
CSF	Cerebrospinal fluid
WM	White matter
GM	Gray matter

List of Figures

1 Introduction

For patients diagnosed with Glioblastoma multiforme (GBM), there is a predefined set of treatments with palliative character preceding a death in less than two years [1]. The reason why it is immune to standard therapeutic interventions is its heterogeneity from the microscopical approach (formation of necrotic regions, microvascular proliferation) and genetical approach (mutations and amplifications of DNA [2]. The treatment begins with resection of the majority of the pathologic tissue, however due to abnormal diffuse nature of GBM it is almost impossible to resect the whole tumour and that is why the surgical resection is followed by chemotherapy treatment applied till the terminal stadium [3].

In this thesis I present the possible way of inducing the necrosis of tumour cells by exposing them to hyperthermia treatment completed by nanoparticle brachytherapy using the thermobrachytherapy (TBT) balloon, which combines both treatment techniques [4]. The approach was to find a more economical solution which would prolong the life span of patients post-surgically by one to two years without having to resect larger amounts of healthy brain tissue. It has been proved that hyperthermia increases the effect of chemotherapy or brachytherapy treatment. In the temperature range from 39 °C to 48 °C, the human brain tissue is more resistive than heat-sensitive tumour cells, therefore the aim is to heat the possible metastatic residues left after resection [5].

There have been few studies published demonstrating temperature-dependent perfusion models of the head regions during hyperthermia. The results of those which have been performed on animals, show that at higher temperatures, the cerebral blood flow (CBF) increases at temperature range from 39 °C to 48 °C, than slowly decreases after it, due to the damage of tissue caused by ablation [5]. Nevertheless, there are few provided values of perfusion rates for specific tissues of brain.

2 Overview of the current state of the art

2.1 Brain tumours

Brain tumours are classified according to the cell considered as their origin. From glioma cells tumours such as astrocytoma, oligodendroglioma, or glioblastoma may be formed. The tumours of Central Nervous System (CNS) may by equally divided into intraaxial and extraaxial, depending whether the tumours grow from the specific brain cells or from the tissues surrounding the white and grey matter of brain.

Clinical symptoms of brain cancer are mainly intracranial hypertense, resulting from the lack of reserve space of brain tissue enclosed by the skull. The symptoms vary according to the location in the brain. For example, the tumours in frontal lobes are responsible for verbal fluency or memory tasks failures, even for a socially inappropriate behaviour. The tumours located in the temporal lobe may lead to a loss of hearing and the incidence in parietal lobe may cause difficulty of speaking [6]. The growth of intracranial pressure depends on the extension of the tumour, perifocal edema and a blockage of cerebrospinal fluid. The treatment of tumours is always a combination of several treatments, including surgical, radiotherapeutic or hormonal [7]. Radiotherapy of brain and skull is suitable for maximum dosage of 60 Grays. One Gray (Gy) is expressed as the absorption of energy of 1 Joule in volume element of 1kg mass [8].

2.1.1 Glioblastoma Multiforme

. GBM is the most occurring tumour of the CNS, classified as an intraaxial malignant type of brain tumour, characterised by brief and aggressive course. Usually it overgrows through the white matter to the second hemisphere of brain. Survival factor is 14 to 15 months and it represents 60% of all brain tumours with the astrocytoma origin [2]. Multiple impacts on the incidence of GBM were studied and revealed no correlation with smoking, diet, immunological status, or electromagnetic fields, however it did show that factors as younger age or good Karnofsky performance score have tendency for longer survival [9]. The glioma tumours are classified in agreement with the standards of World Health Organisation (WHO) which subdivides them into four groups according to their aggressivity, ability to replicate and mainly their histological profile. Grade I is given to lesions that are easily surgically removed, whereas Grades II to IV indicate malignant

nature and invasivity. GBM are classified into highest Grade IV with the most aggressive character. WHO also specifies nomenclature, symptoms, treatment of gliomas and the survival prognosis. [10]

For the diagnosis of CNS tumours, the option of non-invasive imaging method by Computed Tomography (CT) or Magnetic Resonance Imaging (MRI) is proposed or invasive method via catheter angiography MRI. The CT scans are used for cases when patient has metal implants such as pacemakers, however the gold standard of imaging brain tumours is magnetic resonance due to its ability to visualise the soft tissues in higher resolution. T1-wighted MR scans show hypointense lesions, on the other hand, T2-wighted MR scans are used to visualise hyperintense lesions. Applying gadolinium contrast substance can show necrosis of tissue and white matter edemas. Single photon emission computed tomography (SPECT) and positron emission tomography (PET) are used as imaging techniques during therapies to better visualise the changes induced by the chosen treatment technique and to differentiate between tumours that are active and the ones that are responding to interventions [11].

According to the published study [12], the most common incidence of GBM are in frontal lobe with the incidence of 43%, temporal lobe (28%) and parietal lobe (25%). This study also revealed that the tumours usually occur in the right hemisphere and that men have a higher probability of GBM incidence than women.

Treatment of GBM

First step of standard care is the optimal surgery, which means that the maximum size of tumours is resected (usually with 2 to 3 cm of the margin). If the surgery is not possible, biopsy is performed. Due to the massive invasiveness of the tumour, the surgical resection is not referred as a curative treatment since the tumour cells still remain in the surrounding tissue, which leads to the cancer progression and recurrence [7]. Next treatment is the radiotherapy (RT) with the dosage 1.8 to 2 Gy daily, 5 times a week, reference dosage is 60 Gy for patients younger than 70 [13]. RT is followed by 6 cycles of chemotherapy using temozolomide (TMZ) with side effects of headache, nausea and fatigue [3]. However, the study [14] published in 2016 found out that 50 % of patients are not responding to TMZ treatment as GBM cell lines contain TMZ-resistant cells associated with levels of expression of DNA alkylating proteins. To select the correct drugs for a patient, protein or gene profile is required as part of the treatment plan.

2.2 Hyperthermia treatment of malignant tumours

There are two approaches of heating, one is a whole-body hyperthermia, further divided to fever-induced or applied from outside source. The source of heating may be as primitive as steam or hot water or complex as radiation energy. For any heating there is a strict physiological limit of 48 °C, above which cytotoxic changes occur [15].

The most effective hyperthermic treatment is achieved in tissues poorly perfused, where there is different cooling gradient of healthy tissue and tumour tissue by blood flow. Factors that sensitize the tumour to hyperthermia therapy are its acidity, hypoxia, and its lack of nutrients [8]. As the blood plays the major role in heat dissipation, tumour becomes more vulnerable as they have less effective cooling system. The result of hyperthermic application on cell is the change of pH of inner environment, subsequent activation of lysosomal enzymes, slowing down of repetition processes and after the next application of the treatment there is a lethal damage to the cells, usually after combining the treatment technique with adjuvant treatments which is most often a radiation. Combination with chemotherapy may however lead to increase in toxicity, that is why it is disputable to combine these two methods. Implementation of adjunctive hyperthermia to radiotherapy lowers the overall dosage which means it reduces its toxicity [16]. In 2011, the study of Maier-Hauff in Germany received the approval from European Union for the clinical study of applying magnetic iron oxide nanoparticles with heating effect, combined with external stereotactic radiotherapy for the treatment of GBM. Results of the study showed the direct correlation of overall survival with the tumour size and it was proven that the combination prolonged the overall survival in two years. [17]

2.2.1 Impact of hyperthermia on perfusion of tissues

When calculating the distribution of temperature in tissues, usually the change of perfusion is neglected even though it has been proven by several studies that the overall blood flow is dependent on temperature. It is believed that that the blood flow increases during hyperthermia to lead away the hot blood therefore, to cool down the tissue. [18] There have been only few studies performed to find out the specific values of perfusion rate in brain tissues during localised hyperthermia. Experiments that were performed on monkeys and dogs showed that regional cerebral blood flow increases according to the specific temperature and the duration of hyperthermic treatment.

During hyperthermia, the heat span of 41 °C to 45 °C has been proven to create a significant increase in the perfusion of muscles, skin, and fat. On the other hand, the cells of tumours are very vulnerable to even a slight rise of temperature and their blood flow decreases dramatically when heated. After reaching the temperature of 45 °C, the perfusion in normal tissue is decreased. It is believed that this drop occurs after the tissue is damaged due to the heat stress. Assuming constant-rate perfusion and healthy cardiac system of the patient, following curves describe the changing perfusion of the chosen tissues with rising temperature. In *Figure 2.1*, we can observe that muscles have bigger capacity of blood flow than fat and the perfusion of tumour is dramatically decreasing after reaching the temperature of 40 °C. [5]

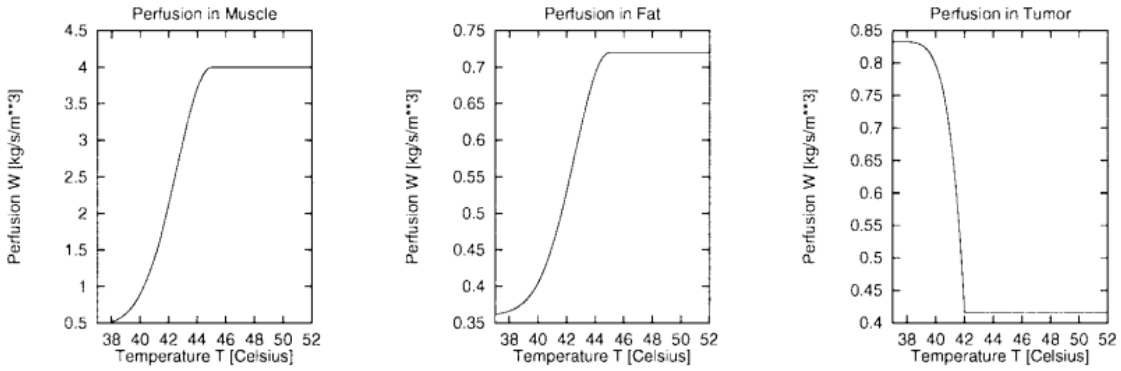

Figure 2.1: Perfusion of muscle tissue, fat and tumour during hyperthermic conditions, taken from [5]

In 1983 Milligan and co. made an experiment that was based on measuring blood flow in canine muscles under hyperthermic conditions using a Laser Doppler Flowmetry as the mean of determination. 25 dogs underwent one hour of heating to the temperature of 43 °C. The results revealed that there were two peaks of blood flow. One after 10 minutes showed an increase from the baseline of 26,9 ml/min/100 gm to 39 ml/min/100gm. and the latter after 40 minutes to 47,6 ml/min/100gm. However, this study dealt with muscle tissues only. [19]

Another study that was performed on new-born pigs examined changes of CBF and metabolic rate of oxygen in response to hyperthermia. Body heating to the temperature of 42 °C marked an increase in CBF by 23 % and a 24% increase in metabolic rate of oxygen. Other factor that was studied during this experiment was the dilatation of vessels during heat stress. It showed that after injecting constrictor (indomethacin) there was a

decrease in CBF by 10%. This showed the responsivity of the dilated cerebrovascular bed to a constrictor stimulus even under hyperthermic conditions. [20]

The study performed on 15 monkeys used interstitial microwave hyperthermia and investigated regional CBF in white matter-The values were obtained using hydrogen clearance method. Increasing temperature from 35,9 °C to 44,7 °C resulted in a rise of regional CBF from 37,7 ml/100 gm brain/min to 82,1 ml/100 gm brain/min. At the temperature of 42 °C that was held for 40 to 60 minutes the peak value of 2,6 times a preheating value was reached in 40th minute with a subsequent decrease to the control value. The study demonstrated that with every 1°C there is a 10% rise in regional CBF. However, exposing the healthy tissue to the temperature higher than 43 °C for more than 40 minutes resulted in vascular damage including haemorrhage and endothelial degeneration. [21]

2.3 Radiotherapy

The impact of radiotherapy on the mean survival rate of patients is undoubtful and currently, it is the most effective method in a complex treatment of brain tumours. Radiation may be applied to the brain by several ways. The most frequently used is the external radiotherapy aiming to maximize the dosage to the tumour and to minimalize the dosages to the surrounding tissue. The radiotherapy tactics is modified according to the histology diagnosis of brain tumour. For example for primary brain tumours with tendency to form metastases to liquor pathways (medulloblastomas), not only brain is radiated but spinal cord as well [22].

Stereotactic radiosurgery, differing from conventional radiotherapy, represents single application of high dosage of radiation. Its beams are concerned into calculated point with desirable biological effect delivering minimal damage to the healthy tissue. The source of radiation may be gamma knife or linear accelerator. Clinical applications are mainly for patients with metastases like meningiomas or schwannomas, tumours of hypophysis [23].

According to the overall body area treated, we distinguish two types of radiotherapy. First one, teletherapy is a method used for applying the radiation dose to almost whole body and is suitable for patients with metastases or vast tumours with risk of spreading to lymphatic system. The second one is brachytherapy which provides the capability of

applying dose in shorter period of time and the risk of damaging the surrounding tissue is minimalised. It is used for treatment of smaller, well emarginated tumours [23].

2.3.1 Brachytherapy

Brachytherapy is divided into three most frequently used techniques. The first one is interstitial brachytherapy represented by the set of needles inserted directly to the tumour bed which delivers high dose rate radiation from the machine called afterloading working with several types of radio-isotopes, most frequently used are Iridium 192, Caesium 137 or Cobalt 60. The machine protects the doctor and personnel from the unwanted dose of radiation. Doctor applies the source from the afterloading to the catheter leading to patient and leaves the room. Nowadays, mainly automatic afterloading machines are used. This type of technique is mostly used for the prostate cancer, breast cancer or for tumours in the neck and head region, as well. The second technique is intracavity brachytherapy during which the source of radiation is placed in body cavities or resection cavities. This technique is often used for gynaecological tumours in vagina, uterus, or oviduct. Another type is intraluminal brachytherapy where the radiation source is applied to hollow tube organs treating the cancer of oesophagus, lungs, or bronchi. During the procedure, silicone pipe is applied into airways to stretch the bronchi narrowed by the obstruction. The procedures may be taken under full or partial anaesthesia [24].

It is important to differentiate between three types of brachytherapy implants. First group are the brachytherapy seeds used as permanent implants, which are loaded with radiation dose that gradually weakens throughout the certain period of time. For the patients with the permanent implant it is necessary to stay away from other people during the period of treatment, this applies mainly for the weakened group – children and pregnant women [25].

The vast group forms the Low Dose Rate (LDR) brachytherapy. This radiation technique operates with doses of 0.2 to 2 Grays per hour. The radiation takes up to two days. It is often used for tumours of prostate, oral cavity, or sarcomas. On the other hand, during High Dose Rate (HDR) brachytherapy, the radiation dose of at least 12 Gy per hour is applied. It is more effective, and it takes only 10 to 60 minutes [26].

3 Aims

Aim of this thesis is to find out the dissipation of heat in the vicinity of thermobrachytherapy balloon. The first step is to design the positions of the TBT balloons in 2 cranial models according to the research on the most common incidence of GBM.

Considering the head model, heating technique and the structure of the TBT balloon, following steps will be taken to simulate each possibility of heat distribution around the resection cavity:

- Calculation of heat generation rates for every size of the balloon filled by nanoparticles
- Simulations in MIDA models
    - Heating by nanoparticle layer in 2-coat TBT balloon
    - Heating by nanofluid in single-layered TBT balloon
        - Heating in hyper-perfused tissue
        - Heating in normo-perfused tissue
- Simulations in patient model
    - Heating by nanoparticle layer in 2-coat TBT balloon
    - Heating by nanofluid in single-layered TBT balloon
    - Heated constantly at temperature from 40 °C to 50 °C without the use of nanoparticles

Results of simulations will be analysed, and heating options will be reviewed according to the ability to heat 5 mm of annular rim of tissue around the resection cavity to the therapeutic temperature range from 39 °C to 48 °C.

4 Methods

4.1 Thermobrachytherapy

This thesis is based on the study [4] in which the treatment option combining hyperthermia with HDR brachytherapy is proposed using thermobrachytherapy balloon (*Figure 4.1*) which is left in the resection cavity right after the surgery. The balloon is made of silicone shaft approved by Food and Drug Administration (FDA) and moulded balloons of different diameters depending on the size of resected area. From the balloon several catheters are conducted. The aim is to treat 5 mm of annular rim of tissue that is at risk of creating metastatic deposits by producing rapid heating (more than 0.2 °C per second) at frequency of 168 Hz with the combination of brachytherapy treatment. The induction heating system is made up of coil with a current density of 5.7 $kA \cdot m^{-1}$ delivering uniform heat to the magnetic nanoparticle layer of 0.6 $W \cdot ml^{-1}$. The experiment was simulated using COMSOL Multiphysics platform and showed satisfying results. The 5 mm annular rim of tissue around resected area was heated to the therapeutic 40 °C to 48 °C and the radiation dose to the tissue delivered was enforced, therefore LDR radiation is effective at such conditions as well.

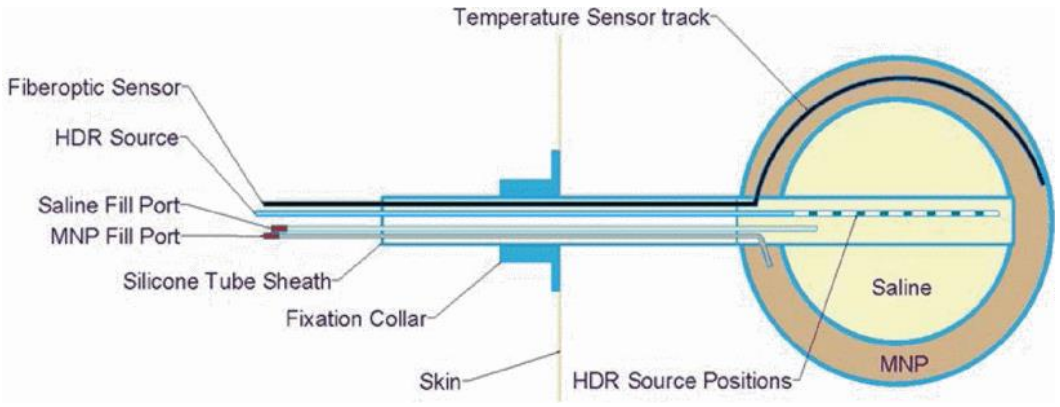

Figure 4.1: Thermorachytherapy balloon used for coupling hyperthermia and brachytherapy treatment [4]

4.2 MIDA model

This model of a 29-year old woman was obtained by 3 modalities of 3 Tesla MRI scanner. Structures such as bones, white and grey matter, eyes, or ears were obtained using T1- and T2-weighted MR images. The arteries and veins of the head and neck were acquired by phase-contrast MR angiography and finally the fibrous character of the tissue was achieved using diffusion tensor imaging of the water in brain. MIDA is made up of 115 structures including all cranial nerves, veins and arteries, detailed structures of CSF, WM and GM, salivary glands or 30 muscle groups [27]. Such complex model offers an opportunity to examine the effect hyperthermia has on the various tissues

4.3 Model of patient

Model of patient is composed of 6 structures including skin, skull, white and grey matter, cerebrospinal fluid, and air. Simulations and calculation of heat distribution are therefore simplified and take less time to evaluate the impact on surrounding tissues. As well as in the MIDA model, each of these structures have specific thermal properties assigned from the library of body tissues [28].

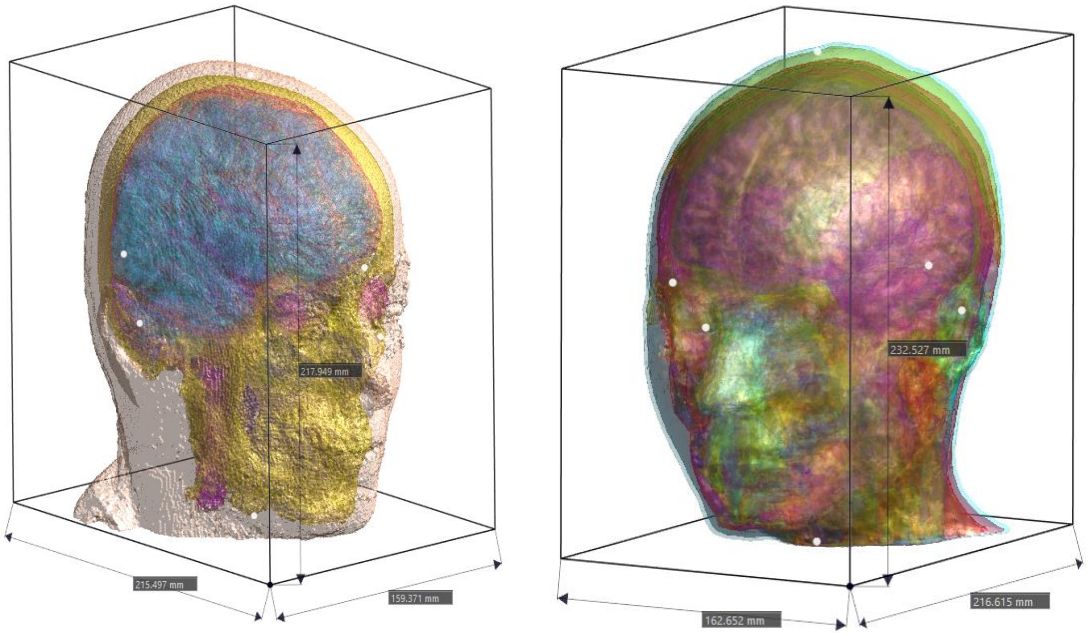

Figure 4.2 Size and structures of patient's head model (*left*) and MIDA [27] (*right*)

4.4 Implementation of Iron (III) Oxide nanoparticles to the heating system

In agreement with my supervisor, this thesis continues the work of Vojtěch Adam, who performed numerical simulations in COMSOL Multiphysics environment using the thermobrachytherapy balloon located in a simplified model of head made up of bone and brain tissue. For heating of nanoparticle-filled balloons, an electromagnetic induction coil of current density 5.79 $kA \cdot m^{-1}$ and frequency of 100 kHz was used. Simulations that are calculated in this thesis are using values of total power loss absorbed by the TBT balloon, which were obtained in the mentioned thesis. These calculations considered both single and double coating of the TBT balloon. It has been proved that using a variation of saline and ferrite magnetic nanoparticles emits more power than in the case of single balloon filled with MNP solution. [29]

As the head model used was rather abridged, these simulations will show how the heating demonstrates on more complex cranial models. Using the values of power loss from Vojtěch Adam's Bachelor Thesis, I calculated Heat Generation Rate (HGR) of nanofluid in TBT balloon. *Table 1* lists HGR of 1-coat balloons, *Table 2* summarises the values for 2-coat TBT balloon. Since in the thesis of Adam, there were only 2 positions of balloons (in the frontal lobe and in the parietal lobe), the values for the temporal lobe were set for the same value as for the frontal lobe.

$$G = \frac{P}{m} = \frac{P}{\rho \cdot V} = \frac{P \cdot 3}{\rho \cdot 4 \cdot \pi \cdot r^3} \tag{1}$$

where G stands for heat generation rate in $W \cdot kg^{-1}$, P is power loss in Watts taken from [29], m stands for mass of the solution in kilograms, calculated as the product of its density ρ in $kg \cdot m^{-3}$and volume V in m^{-3}. The results for each size are summarised in *Table 1*.

Table 1: Calculated values of Heat Generation Rate for the TBT balloon filled only with ferromagnetic nanofluid

Lobe	**Radius of the TBT balloon *r*** (m)	**Power Loss *P*** (W) [29]	**Heat Generation Rate *G*** ($W \cdot kg^{-1}$)
Frontal	0.010	1.467	**346.59**
	0.015	5.531	**387.18**
	0.020	13.838	**408,66**
Temporal	0.010	1.467	**346.59**
	0.015	5.531	**387.18**
	0.020	13.838	**408.66**
Parietal	0.010	1.147	**270.98**
	0.015	4.321	**302.48**
	0.020	10.838	**318.97**

For the double-layered TBT balloons, there is a slight change in formula for calculating HGR. Considering the fact, that the nanofluid is located between two silicone coats of different diameter, the volume is adjusted to the following form:

$$G = \frac{P}{m} = \frac{P}{\rho \cdot V} = \frac{P \cdot 3}{\rho \cdot 4 \cdot \pi \cdot (r_o^3 - r_i^3)} \quad (2)$$

where r_o is radius of the outer balloon in meters and r_i is radius of the inner balloon filled with saline solution. Results are written down in *Table 2*.

Table 2: Calculated values of Heat Generation Rate for double-layered TBT balloon

Lobe	**Radius of the outer TBT balloon r_o** (m)	**Radius of the inner TBT balloon r_i** (m)	**Power Loss *P*** (W) [29]	**Heat Generation Rate *G*** ($W \cdot kg^{-1}$)
Frontal	0.010	0.004	1.565	**556**
	0.015	0.009	6.740	**790**
	0.020	0.014	18.377	**1055.08**
Temporal	0.010	0.004	1.565	**556**
	0.015	0.009	6.740	**790**
	0.020	0.014	18.377	**1055.08**
Parietal	0.010	0.004	1.221	**433.78**
	0.015	0.009	5.254	**616.02**
	0.020	0.014	14.314	**821.81**

4.5 Preparation of simulations

For the values of heat generation rates from *Tables 1 & 2*, simulations of heating from the 1-coat and a 2-coat TBT balloon will be performed. The 2-coat TBT balloon contains additional inside balloon, filled with saline solution (as illustrated in *Figure 4.1*). Between the silicone balloons, a 5mm wide ring of nanofluid is located.

In *Table 3* I state the parameters of TBT balloon's materials used for thermal simulations. The volume concentration of ferrite nanofluid is 2 % and its properties were taken from study dealing with thermal properties of Fe_3O_4 nanofluids under hyperthermic conditions [30]. Saline solution of 0.9 % sodium chloride was used to fill the inner balloon.

Table 3: Parameters used for the materials of TBT balloon

	Silicone [31]	**Fe_3O_4 nanofluid** [30]	**Saline solution** [32]
Mass density ρ ($kg \cdot m^3$)	1250	1079.83	1005
Specific Heat Capacity Cp ($J \cdot kg^{-1} \cdot K^{-1}$)	768	4112.74	4050
Thermal Conductivity λ ($W \cdot m^{-1} \cdot K^{-1}$)	1.59	0.9657	0.6

To compare the simulations that were calculated on tissues with higher perfusion rates, another set of models was created in which the perfusion rates remained pre-set. For the same purpose of comparison, other simulations were computed to depict the heating of patient model from the balloon filled with solution at the temperature of 45 °C constantly heated for 30 minutes.

4.5.1 Positions of TBT balloons

Position of balloons was chosen according to the research on most common lobes affected by the GM [12]. Moreover, the positions of TBT balloons in MIDA head were set so the main veins and arteries are in a close position of them. This way the importance of thermoregulation function of blood vessels is to be examined. More specifically, TBT balloon in the frontal lobe is positioned just below the Superior sagittal sinus of Internal jugular vein. The heat dissipation in the temporal lobe is affected by the Superficial temporal artery and vein and in the parietal region by the Parietal emissary vein and Superior sagittal sinus.

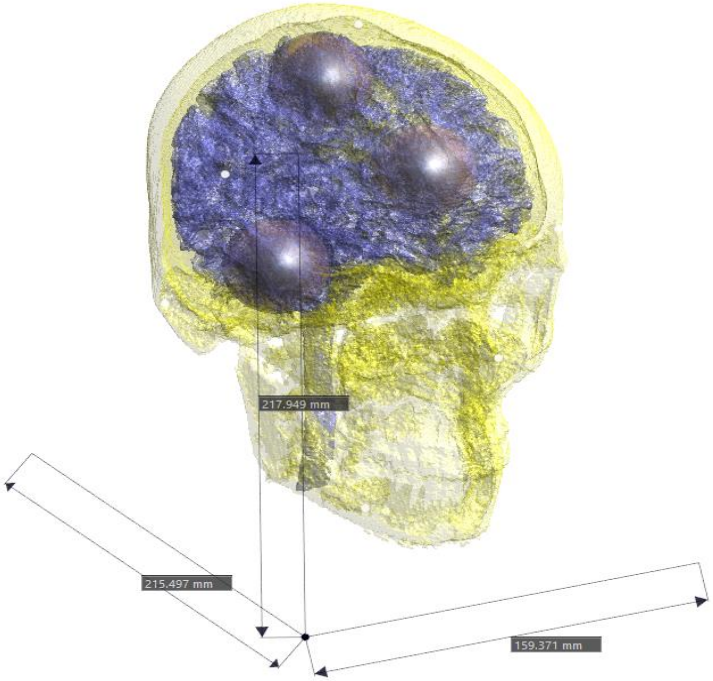

Figure 4.3: Positions of TBT balloons in the model of patient

For every position 3 sizes of TBT balloons were designed. Their diameters are 4 cm, 3 cm and 2 cm set according to the study [4]. Power loss in the balloon of the diameter 1 cm was so small that its heating properties are neglected as it took more than 30 minutes to heat the close environment of the TBT balloon sufficiently [29]. For each location, two graphs are to be constructed. First, showing the temperature distribution in the vicinity of the balloon and later representing the temperature change throughout the time of the simulation 5 mm from the coating of the balloon. Every graph compares three different sizes of the TBT balloon.

4.5.2 Sim4Life platform and setting

Method chosen for the simulation was *Thermal transient* which is a numerical method of analysing heat transfer during a specific period. There are two options for using it. Either to find out the time at which the thermal equilibrium was achieved or to observe the specific heat dissipation in object at given amount of time. In this thesis both applications will be used. The treatment time suggested is 30 minutes. Our aim is to determine how far can the heat be transferred from the TBT system and at what specific minute will the system reach a constant value of temperature held for the rest of the simulation. Following types of settings are offered:

Setup: Overall time of simulation and the heating model is configured. Time of every simulation was estimated on 30 minutes (1800s) and the Pennes heating model was applied.

Materials: 39 types of materials in MIDA and 6 materials for patient model are assigned values of density, thermal conductivity, and specific heat capacity from the database of IT'IS Foundation. For the nanofluid, Heat Generation Rate was adjusted according to the values from *Table 1* and *Table 2*. These values are held constant during whole time of simulation. For the models without the application of alternating magnetic field, the convective temperature for whole TBT balloon was set to specific risen temperature from 40 °C to 50 °C. Hyperperfused models are considering different parameters of Heat Transfer Rates which were set to Piecewise-Linear with assigned linear coefficients, perfusion and temperature ranges of values specified in Table X.

Initial conditions: This temperature condition refers to the start value assigned at the beginning of the simulation. Two sets of initial condition settings were chosen, the first one being the overall temperature of the environment of 25 °C. For every body tissue, the temperature of 37 °C was applied and for the cases of simulations where the heating is applied from the hot-fluid balloons, the initial condition of the balloons were set to a value between 40 °C and 50 °C. Otherwise, the TBT balloon's initial state was same as the temperature of other tissues in both cranial models.

Boundary Conditions: This condition specifies how the thermal model behaves at boundaries between the structures. There are three types of this condition:

- Dirichlet: It fixes the surrounding tissue or environment to the unchanging value in degrees of Celsius.

- Neumann: Fixes Heat Flux value to the unchanging value which indicates how much heat is either lost to the environment or gained by the surrounding tissues.
- Mixed: The third type combines the previous two and is expressed by three values: temperature, Heat Transfer Coefficient and Heat Flux which is calculated as the product of heat transfer coefficient and temperature difference between 2 tissues or between environment and tissue.

Mathematically, mixed boundary condition can be expressed using following set of equations:

$$F_{boundary} = k \cdot \frac{dT}{dn} + h \cdot (T - T_{outside}) \tag{3}$$

where k is thermal conductivity in $W \cdot m^{-1} \cdot K^{-1}$, T is the temperature of the object that emits heat, n is the thickness of the wall in meters, h is heat transfer coefficient in $W \cdot m^{-2} \cdot K^{-1}$, $T_{outside}$ is the temperature of the environment. Heat flux caused by radiation heat from a small object to the environment is given as:

$$\sigma \cdot (T^4 - T_{outside}^4) \tag{4}$$

where σ is Stefan-Boltzmann constant ($5.67 \cdot 10^{-8}$ $W \cdot m^{-2} \cdot K^{-4}$), T is temperature of the small object and $T_{outside}$ is the temperature just beyond the wall of the object.

Formula can be rewritten as the product of following temperature equations:

$$\sigma \cdot (T - T_{outside}) \cdot (T + T_{outside}) \cdot (T^2 - T_{outside}^2) \tag{5}$$

for smaller temperature differences between object and wall, equation (5) can be transformed into following form:

$$4 \cdot \sigma \cdot (T - T_{outside}) \cdot T_{outside}^3 \tag{6}$$

For the models with balloons filled with hot saline, the mixed boundary condition was applied to the layer of outer silicone to provide heat transport to the surrounding tissue with the value of Heat Transfer Coefficient 10 $W \cdot m^{-2} \cdot K^{-1}$ and corresponding Heat Flux value. The third condition was applied to the environment as well, to minimalize the heat

loss through the skin. For this reason, the Heat Transfer Coefficient was set to 10 $W \cdot m^{-2} \cdot K^{-1}$ and the calculated value of Heat Flux is 120 $W \cdot m^{-2}$ (Heat Transfer Coefficient multiplied by the difference of outside temperature 25 °C, and the skin tissue temperature, 37 °C).

Sensors: In this setting option we can set the number of intervals at which the simulation will be captured. The number divides the overall simulation time evenly. Analysing the final results, we can see the gradual change throughout the time in a set of horizontal, sagittal or frontal slices. The simulations were captured in 8 time points.

Grid and Voxel settings: The size of each voxel (three-dimensional volume pixel) (is configured with the emphasize on the boundaries of each different structure. It is essential to establish the priority of structures that are overlayered. In this case the TBT balloon must have higher priority number than the tissue in which it is inserted. The structures of TBT balloon are prioritised in the following order outer balloon, ferromagnetic nanofluid layer, inner balloon, saline solution, respectfully.

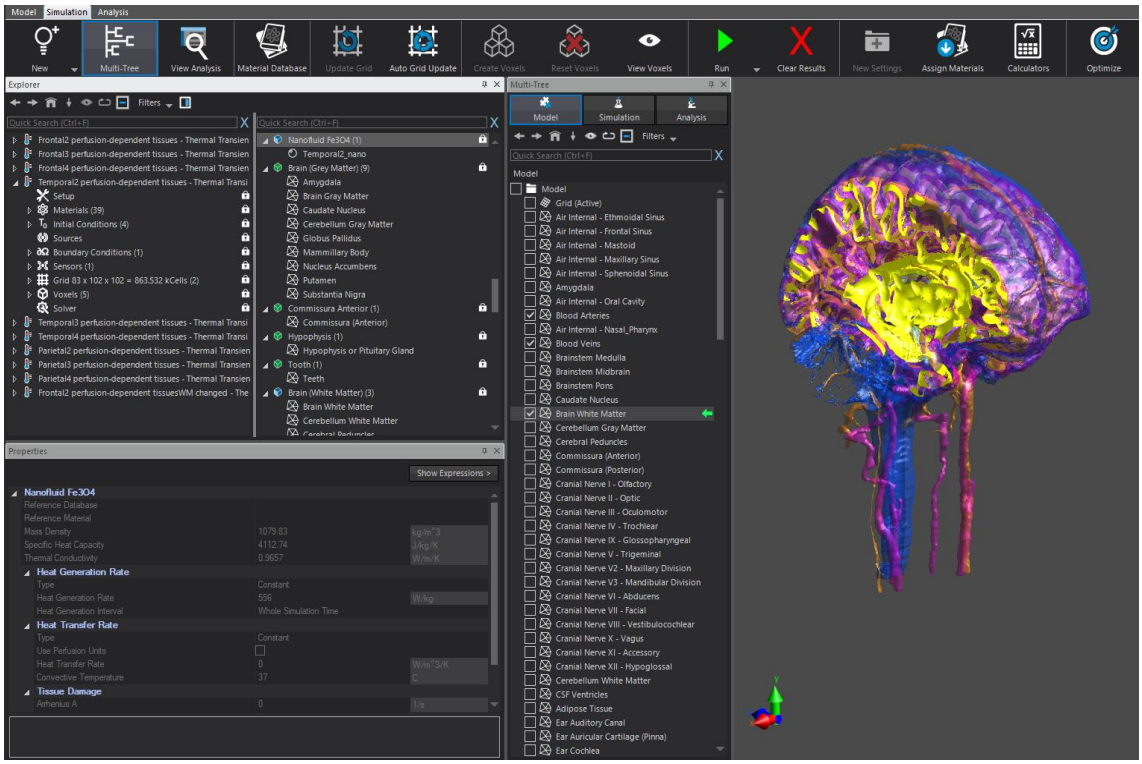

Figure 4.4: The simulation tab in the Sim4Life environment

After the simulation is finished, the analysis of results is possible using *Slice viewer* option of sensor extractor. Slices can be viewed in three cross-sections: coronal (frontal), mid-sagittal (medial), or horizontal. For each slice there is a possibility of animation of heat generation throughout the simulation time. At chosen time, there are two option for line extraction of temperature dependence, either the *Spatial mode* which illustrates the graphical layout of temperature at chosen direction of cross-section or *Temporal mode*, which depicts the behaviour of temperature at chosen point throughout the simulation.

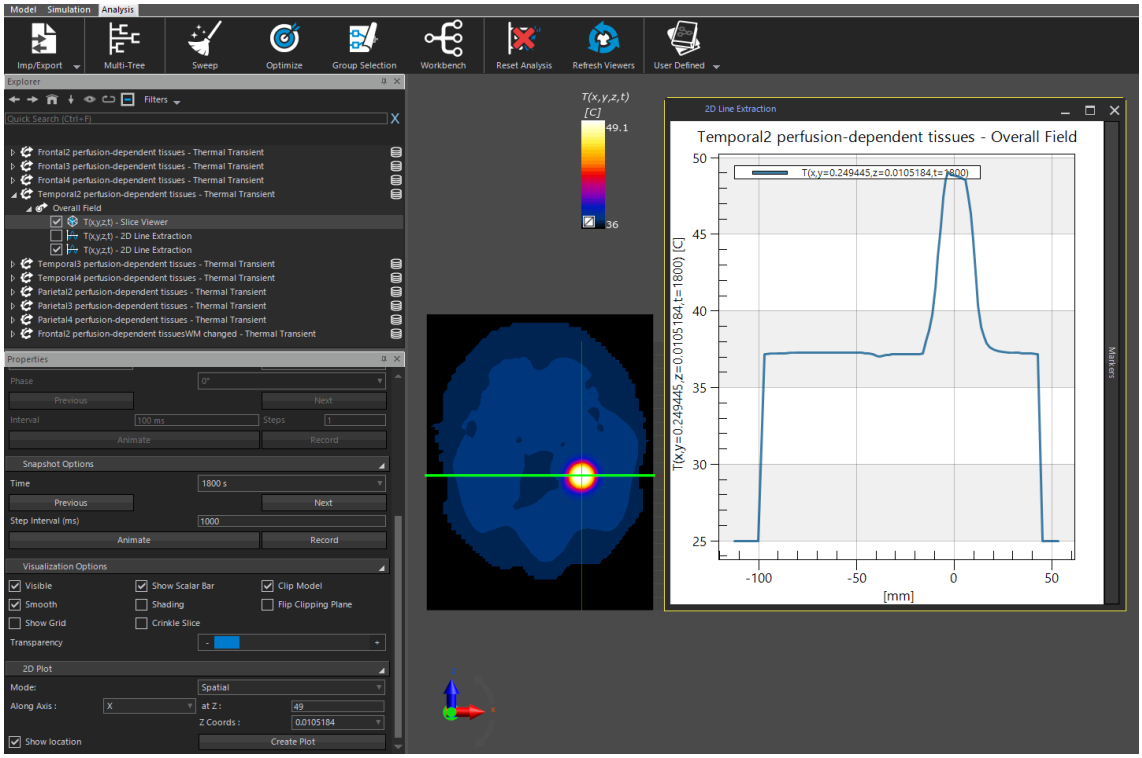

Figure 4.5: The analysation tab in the Sim4Life environment, proposing the options for slice viewer (*bottom left)* and the line extraction of temperature dissipation (*right*)

Both mentioned modes will be used to analyse the temperature distribution in the vicinity of the TBT balloons positioned in three cranial lobes. For Spatial mode, the distribution of temperature will be drawn across horizontal section at lateral dextral-sinistral line leading through the centre of TBT balloon. For the temporal mode, the progression of temperature will be depicted at the point exactly 5 mm from the coating of the balloon. The aim of TBT system is to heat 5mm rim of tissue in which the potential metastatic residue may occur after the resection of tumour.

4.6 Implementation of perfusion

Part of the thesis is implementation of perfusion of tissues during hyperthermia. Sim4Life has pre-set values of perfusion rates for every biological material, however these values need to be adjusted to meet the hyperthermic conditions during which the blood flow changes. From the research summarised in *Chapter*, I used following adjustments to the perfusion: As was mentioned above, there has been only few studies on this subject and as the TBT balloons were located in the white matter, it was essential to change this tissue. In the study on thermobrachytherapy, the perfusion of white matter was doubled from the baseline [4]. Much more perfused grey matter has a perfusion rate of 763.67 $ml \cdot min^{-1} \cdot kg^{-1} \cdot K^{-1}$. From the study [5], I adjusted the perfusion rates for the tissues of fat and muscles The perfusion change was applied for the temperature range from 37 °C to 48 °C.

Perfusion of muscle, fat and tumour tissue is expressed by following equations stated in [5]:

$$W_{muscle} = \begin{cases} 0.45 + 3.55 \cdot e^{\left(-\frac{(T-45)^2}{12}\right)} & \text{T} \leq 45\ ^\circ\text{C} \\ 4 & \text{T} > 45\ ^\circ\text{C} \end{cases} \quad (7)$$

$$W_{fat} = \begin{cases} 0.36 + 0.36 \cdot e^{\left(-\frac{(T-45)^2}{12}\right)} & \text{T} \leq 45\ ^\circ\text{C} \\ 0.72 & \text{T} > 45\ ^\circ\text{C} \end{cases} \quad (8)$$

$$W_{tumour} = \begin{cases} 0.833 & \text{T} < 37\ ^\circ\text{C} \\ 0.833 - \frac{(T - 37)^{4.8}}{5438} & 37\ ^\circ\text{C} \leq \text{T} \geq 42\ ^\circ\text{C} \\ 0{,}416 & \text{T} > 42\ ^\circ\text{C} \end{cases} \quad (9)$$

In these formulas, *W* is a mass flow rate of blood and its unit is $kg \cdot s \cdot m^{-3}$. The perfusion units used in Sim4Life are expressed in $ml \cdot min^{-1} \cdot kg^{-1} \cdot K^{-1}$. For conversion of these units, density and volume would be needed, however, from the *Database of Human Tissues* [28], we know the values of perfusion at temperature of 37 °C in $ml \cdot min^{-1} \cdot kg^{-1} \cdot K^{-1}$ and with knowledge of values from *Equations 7–9*, we can easily calculate the perfusion rates at temperature 45 °C by multiplying them by scaling factor.

Table 4: Normal and hyperthermic perfusion rates of chosen tissues

Tissue	**Normal perfusion rate** ($ml \cdot min^{-1} \cdot kg^{-1} \cdot K^{-1}$)	**Hyperthermic perfusion rate** ($ml \cdot min^{-1} \cdot kg^{-1} \cdot K^{-1}$) [5]
White Matter	212.333 [28]	**424.666**
Subcutaneous Fat	32.709 [28]	**65.111**
Muscles	36.738 [28]	**314.67**
Tumour	45 [33]	**22.473**

Even though muscles and fat are not in the direct presence of the heating system, I have chosen them for better dissipation of temperature near the skin. This way, it can be seen whether the head leads away the heated blood from the outer layers. For comparison, the value of perfusion rate for veins and arteries is 10 000 $ml \cdot min^{-1} \cdot kg^{-1} \cdot K^{-1}$ [28]. For this major difference, the impact of the position near vessels will be further analysed.

4.7 Bioheat Pennes equation

This differential equation balances the inner energy of the passive system by blood flow and by preserving the heat in the body. One of the many roles of blood in the body is to transfer heat through arterioles therefore to provide certain heating and cooling system. At hyperthermic conditions, the walls of blood veins and arteries are stretched (vasodilatated). This decrease of vascular resistance causes faster flow and certain amount of heat is evaporated through the endocrine system of skin. It is formulated by the following formula:

$$\rho \cdot C \frac{dT}{dt} = \nabla \cdot (k \cdot \nabla \cdot T) + Q_{bio} + Q_{met} \quad (10)$$

where ρ is density of tissue in m kg$\cdot^{-3}$, C is specific heat capacity in J$\cdot$kg$^{-1}\cdot$K^{-1}, T is temperature in Kelvins or degrees Celsius, t is time. ∇ is nabla, differential operator of three-dimensional Euclidean space, k is thermal conductivity coefficient in W$\cdot$m$^{-1}\cdot$K^{-1}. Q_{met} expresses metabolic heat produced by tissue in W$\cdot$m^{-3} and Q_{bio} is heat from the blood perfusion. It is calculated as:

$$Q_{bio} = \rho_b \cdot C_b \cdot \omega_b \cdot (1 - k_e) \cdot (T_a - T) \quad (11)$$

where ρ_b, C_b and ω_b are density, specific heat capacity and perfusion of blood, k_e expresses the non-balanced relation between blood and tissue. T stands for the temperature of surrounding tissue in Kelvins and T_a is temperature in blood vessels.

5 Results

5.1 MIDA model with 2-coat TBT balloons

First set of results is the analysation of heating from double-layered brachytherapy balloon. The perfusion in the MIDA head was adjusted to meet the hyperthermic conditions.

5.1.1 Frontal Lobe

Figure 5.1 represents the temperature distribution in cranial slices at the end of the simulation, which means after 30 minutes. In every following figure depicting the heating system positioned in different brain lobes, the specific location of the slice is shown on the left size (which is always passing through the centre of the TBT balloon). In column (a) balloon with 2 cm in diameter is shown, in (b) a 3 cm and in (c) a 2 cm TBT balloon.

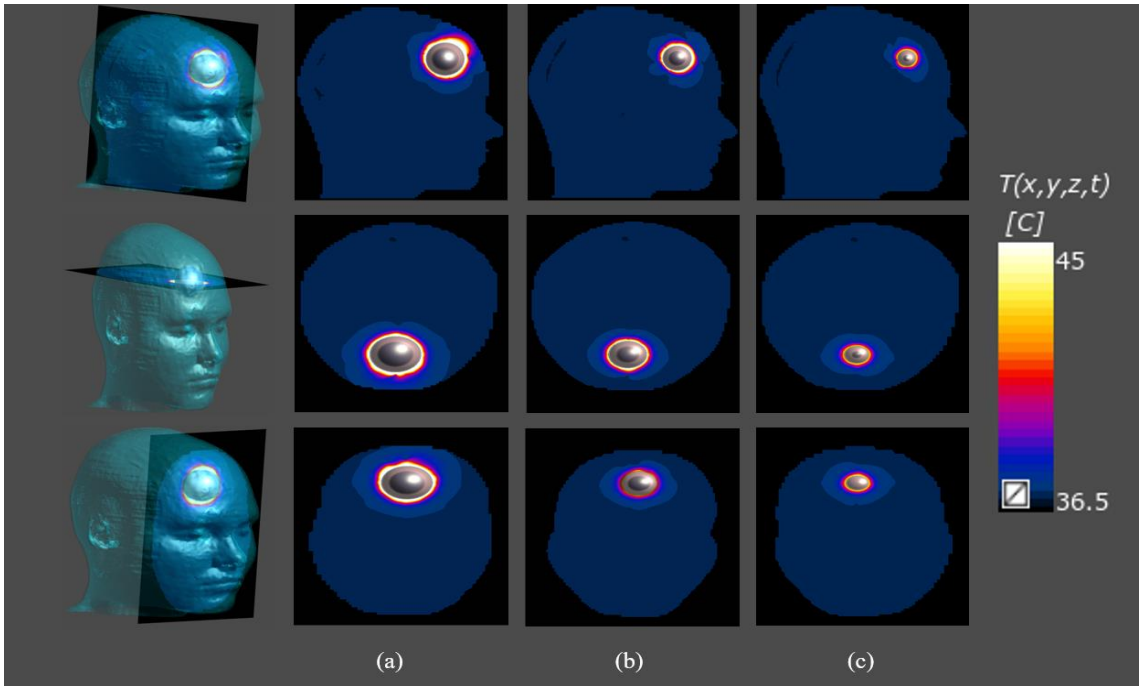

Figure 5.1: Temperature layout around the 2-coat TBT balloons with a 4 (a), 3 (b) and 2 (c) -cm diameter located in a frontal lobe of MIDA model displayed in sagittal, horizontal and coronal slice, 1800 s after the start of simulation

To show the specific temperature values, two graphs are constructed for each slice, one representing the temperature distribution from the horizontal section of the brain leading through the centre of the balloon. The temperatures shown are after 30 minutes of simulation. The horizontal section was chosen since it is the slice with most significant changes of temperature as the coil is placed in the horizontal position during the procedure. The second graph shows how the temperature progressed throughout the time. The later graph is shown for the point exactly 5 mm from the outer balloon.

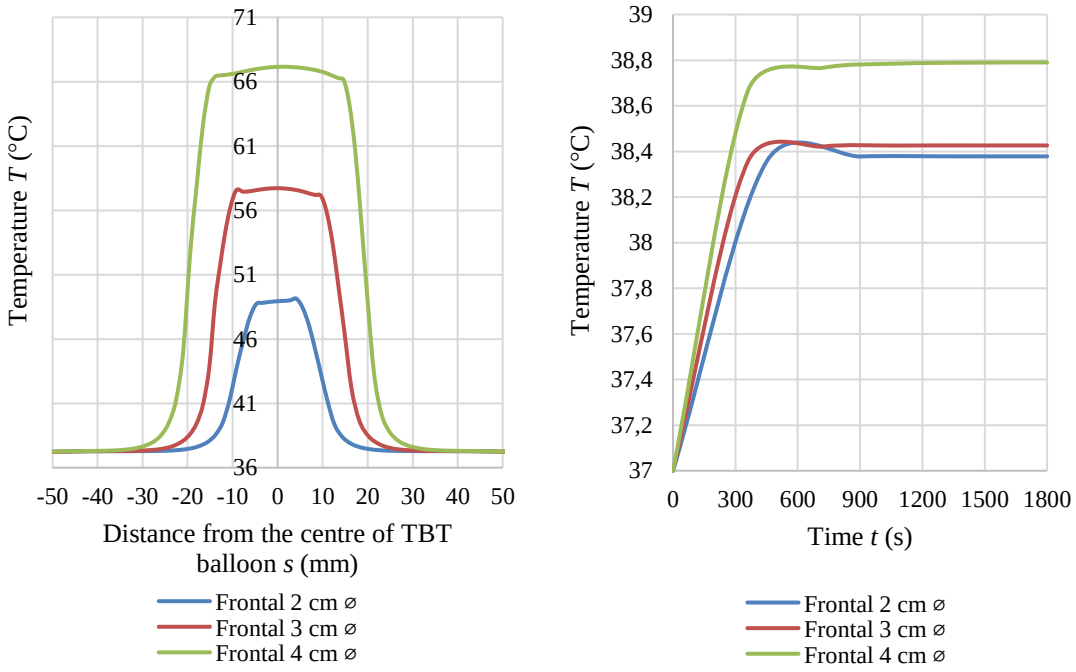

Figure 5.2: Graphical representation of temperature distribution in the 2-coat TBT balloons and in its vicinity (*left*) and the temperature progression throughout the simulation 5 mm from the balloons (*right*) located in frontal lobe of MIDA model

The graph depicting the distribution of temperature shows rather obtuse information about the temperature on the surface of the balloon. For this reason, another graph is presented which zooms in the temperature behaviour from the outer silicone layer of the TBT balloon.

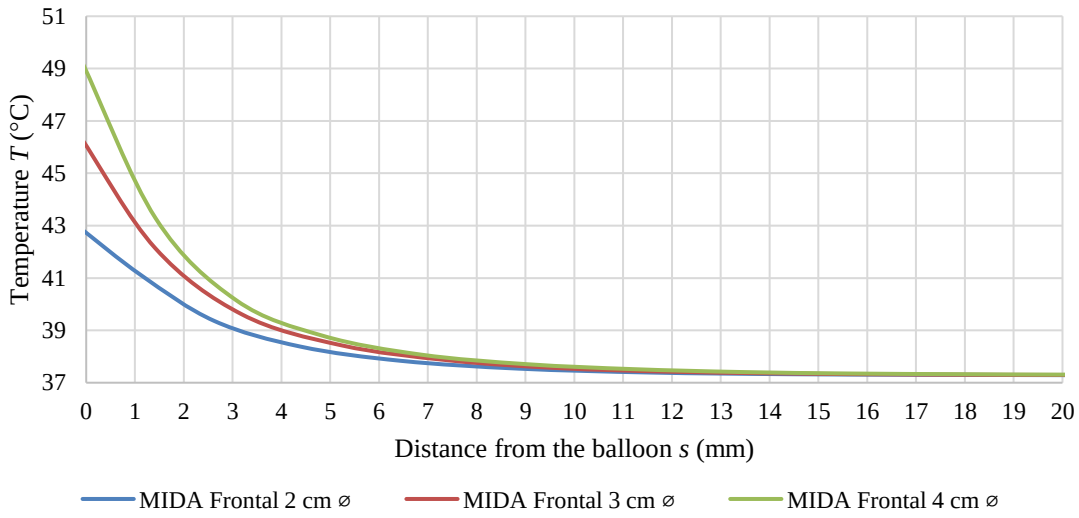

Figure 5.3: Distribution of temperature from the TBT balloons located in the frontal lobe of the MIDA model

For TBT balloons located in temporal and parietal lobe, the same set of graphs was created from the obtained results. *Figures 5.4* and *5.7* are depicting the graphical temperature distribution in tissues at 3 different slices

5.1.2 Temporal Lobe

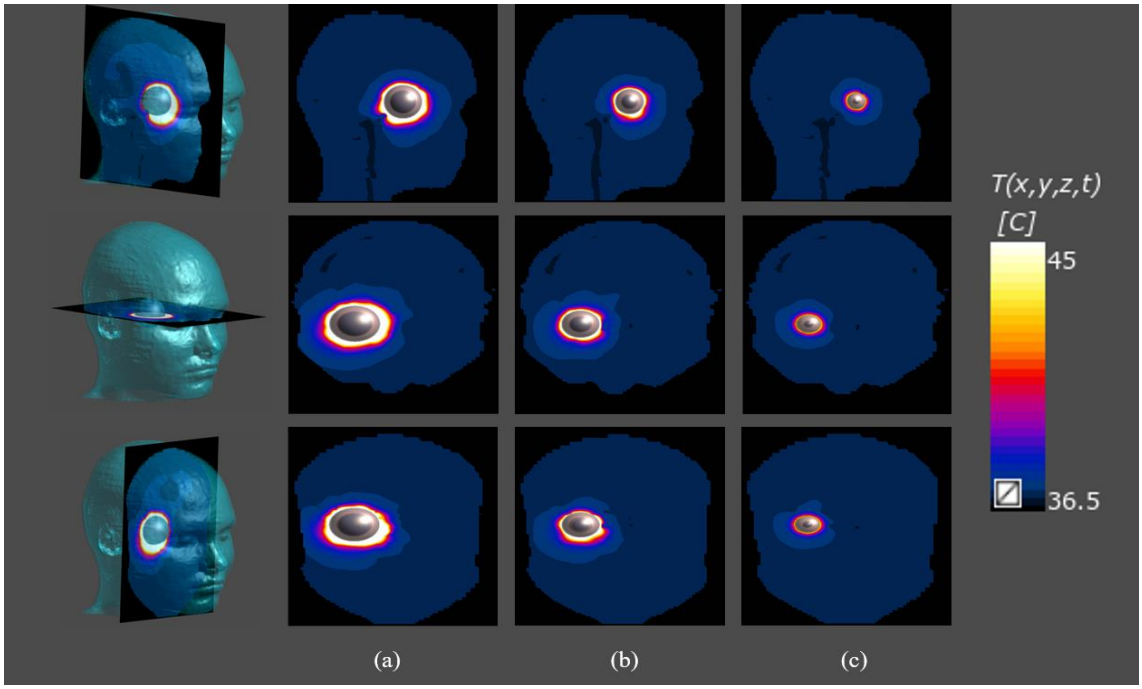

Figure 5.4: Temperature layout around the 2-coat TBT balloons with a 4 (a), 3 (b) and 2 (c) -cm diameter located in a temporal lobe of MIDA model displayed in sagittal, horizontal and coronal slice, 1800 s after the start of simulation

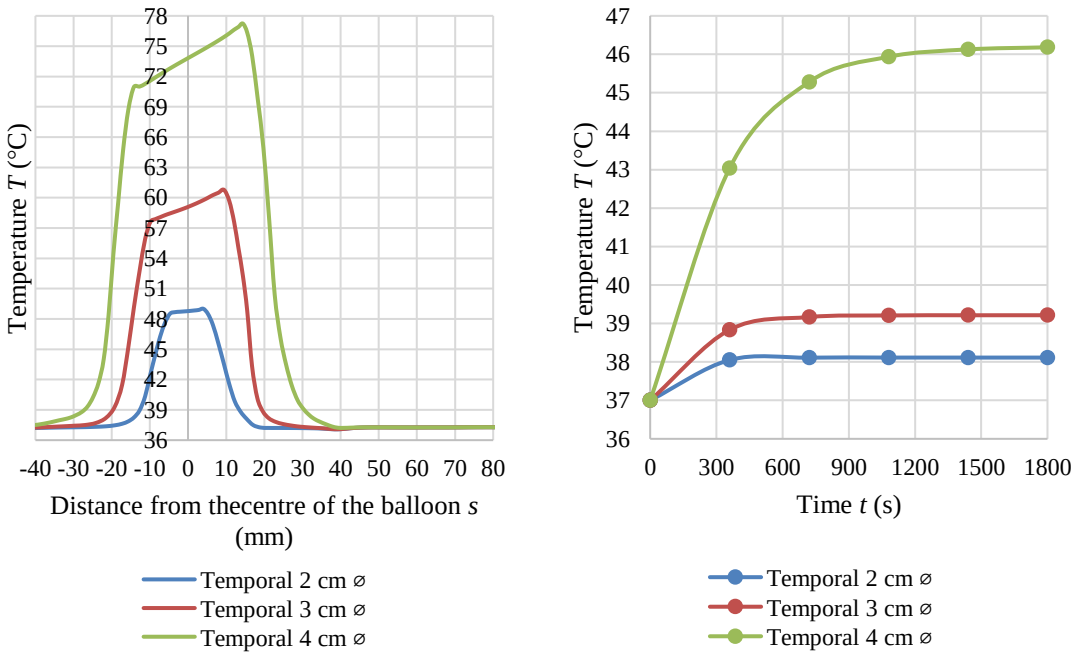

Figure 5.5: Graphical representation of temperature distribution in the 2-coat TBT balloons and in its vicinity (*left*) and the temperature progression throughout the simulation 5 mm from the balloons (*right*) located in temporal lobe of MIDA model

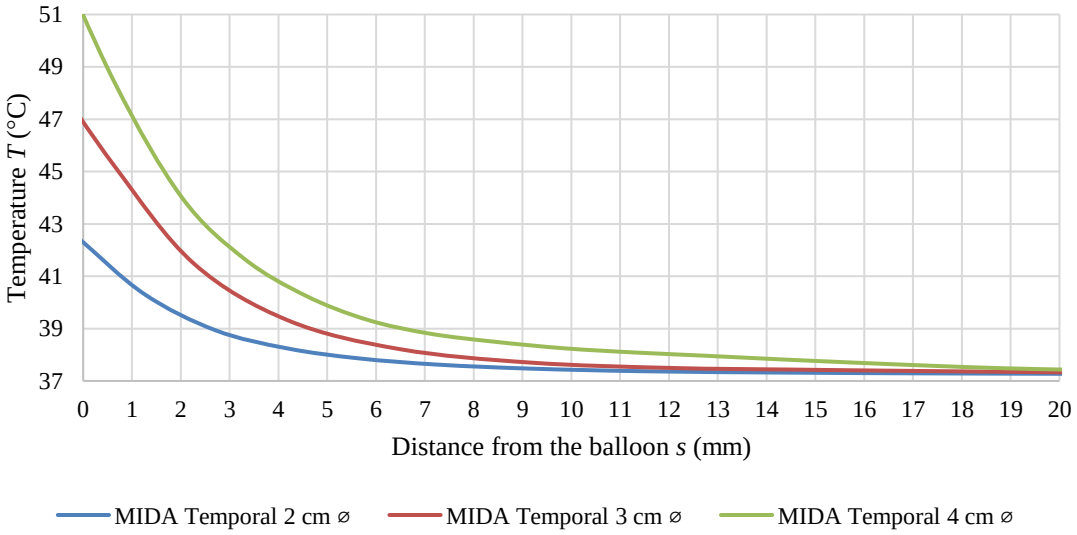

Figure 5.7: Distribution of temperature from the TBT balloons located in the temporal lobe of the MIDA model

5.1.3 Parietal Lobe

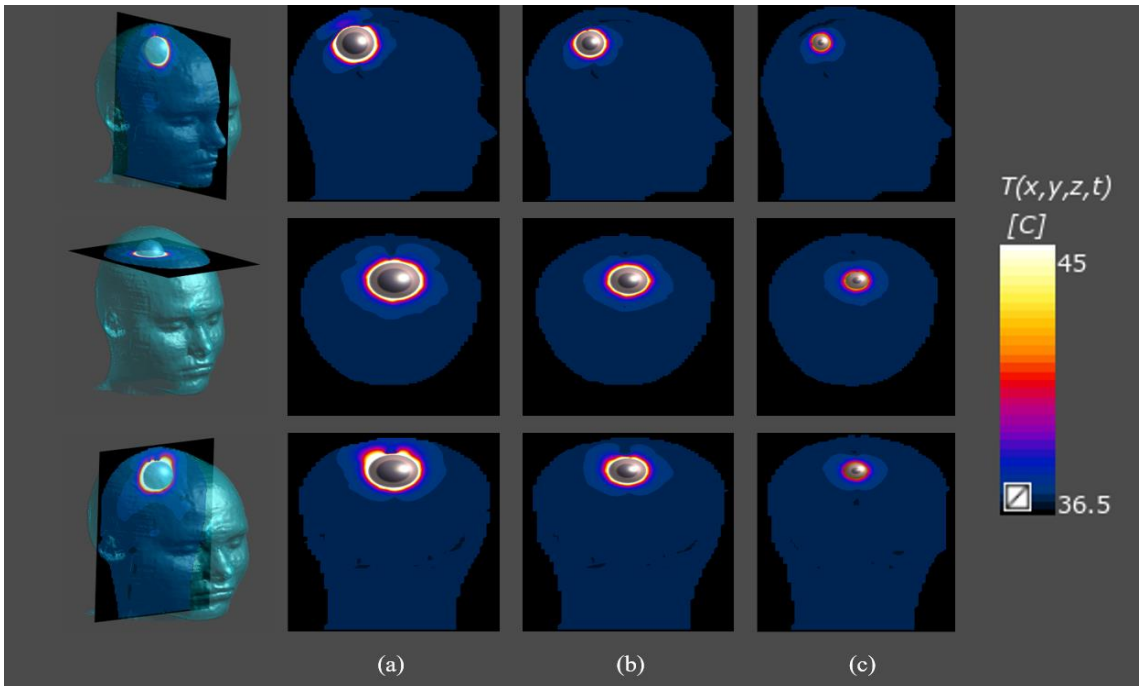

Figure 5.6: Temperature layout around the 2-coat TBT balloons with a 4 (a), 3 (b) and 2 (c) -cm diameter located in a parietal lobe of MIDA model displayed in sagittal, horizontal and coronal slice, 1800 s after the start of simulation

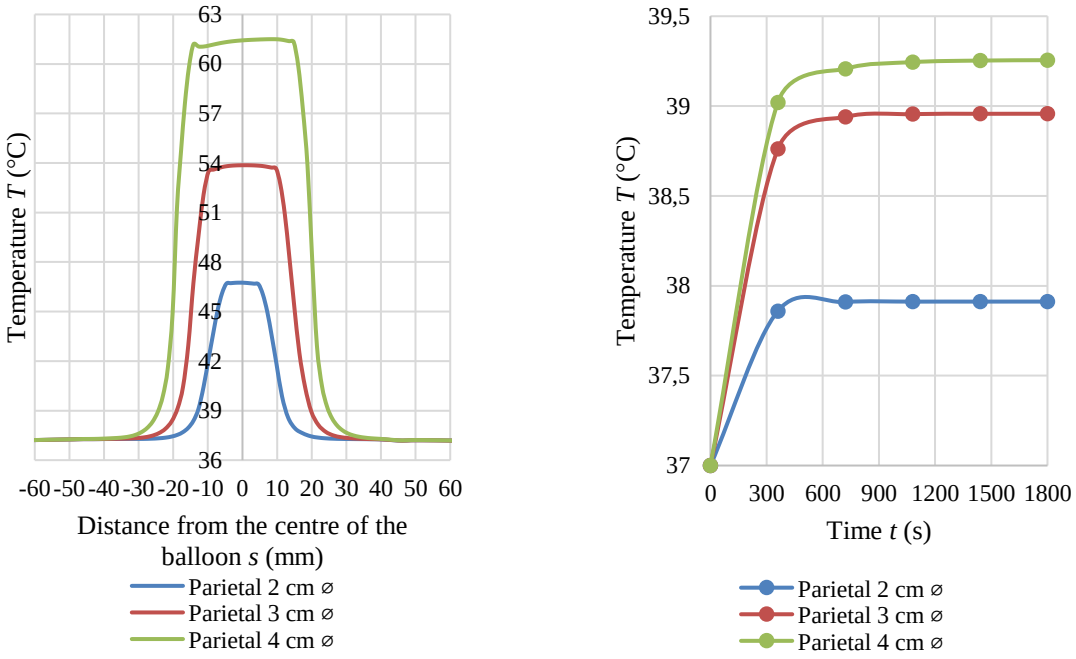

Figure 5.8: Graphical representation of temperature distribution in the 2-coat TBT balloons and in its vicinity (*left*) and the temperature progression throughout the simulation 5 mm from the balloons (*right*) located in parietal lobe of MIDA model

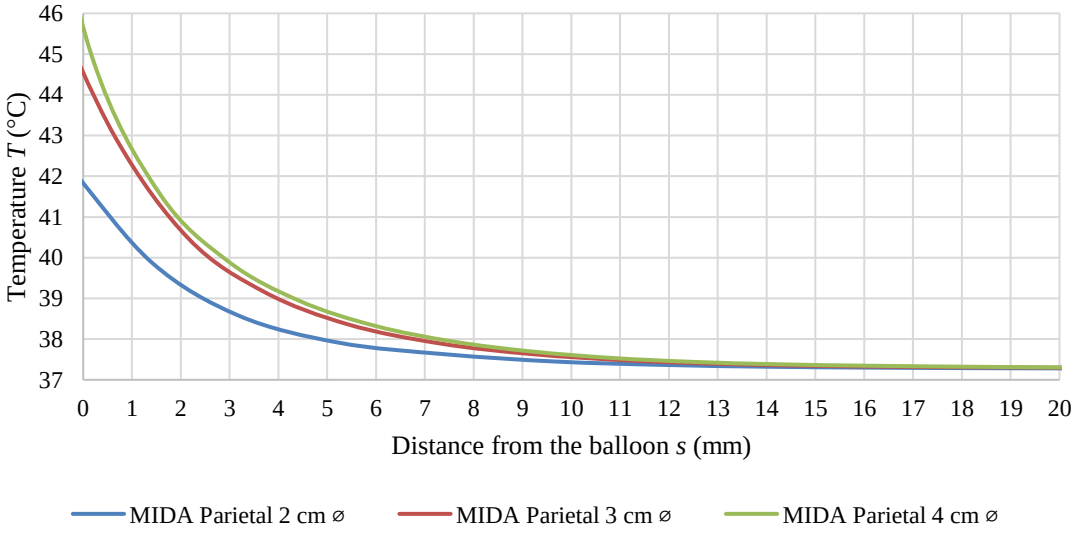

Figure 5.9: Distribution of temperature from the TBT balloons located in the parietal lobe of the MIDA model

The largest TBT balloons in the frontal and temporal lobe heated the tissue excesively beyond the limitation 48 °C. In *Table 5* I state the time in which the tempearture on the surface of the balloons was exceeded.

Table 5: Times at which the temperature on the surface of the 2coat balloon reached 48 °C

Location of the balloon	Frontal lobe (⌀ = 4 cm)	Temporal lobe (⌀ = 4 cm)
Time *t* (min)	5.75	4.08

5.2 Patient head model with 2-coat TBT balloons

The same set of simulations are to be analysed for the realistic model of patient with six tissues. Positions of the TBT balloons were fixed in the same locations as for the MIDA model even though there was not emphasize on the placement near the vessels as this model does not contain them. Each of the nine simulations was set to 30 minutes.

Figures 5.10, *5.13* and *5.16* represent the distribution of temperature in cranial slices dividing the TBT balloons in halves. *Graphs 5.11, 5.12, 5.14, 5.15, 5.17* and *5.18* show numerical values reached during the simulations.

In *Table 6* I specify the times at which the temperatures on the surface of the balloons passed the required limit.

5.2.1 Frontal Lobe

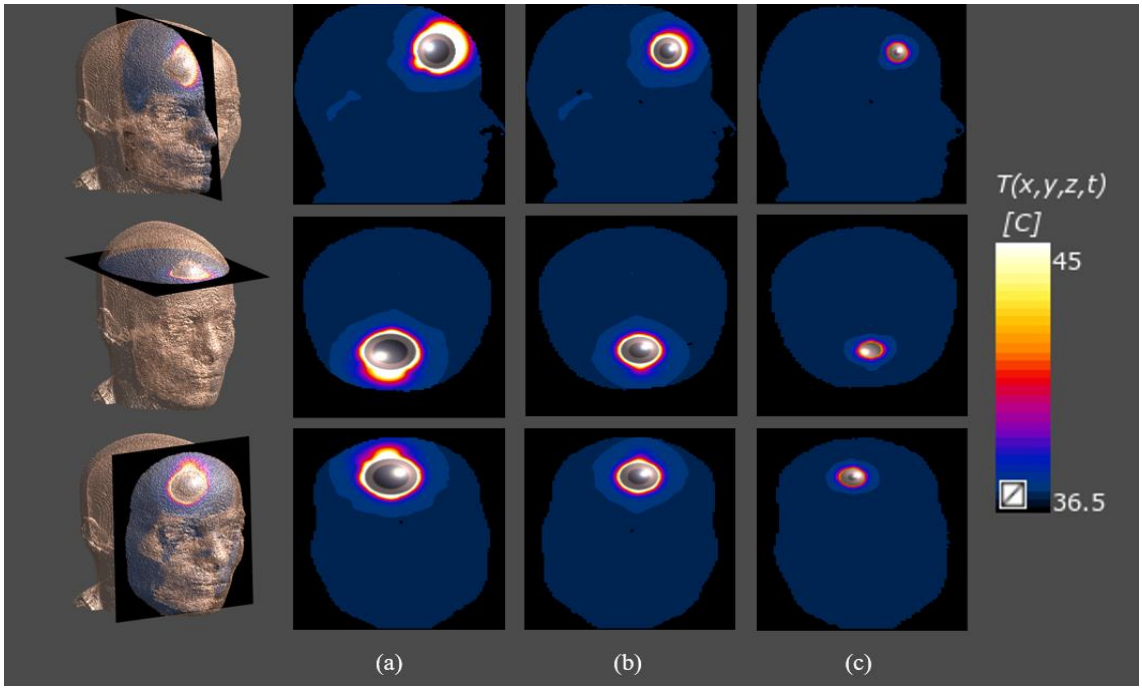

Figure 5.10: Temperature layout around the 2-coat TBT balloons with a 4 (a), 3 (b) and 2 (c) -cm diameter located in a frontal lobe of patient model displayed in sagittal, horizontal and coronal slice, 1800 s after the start of simulation

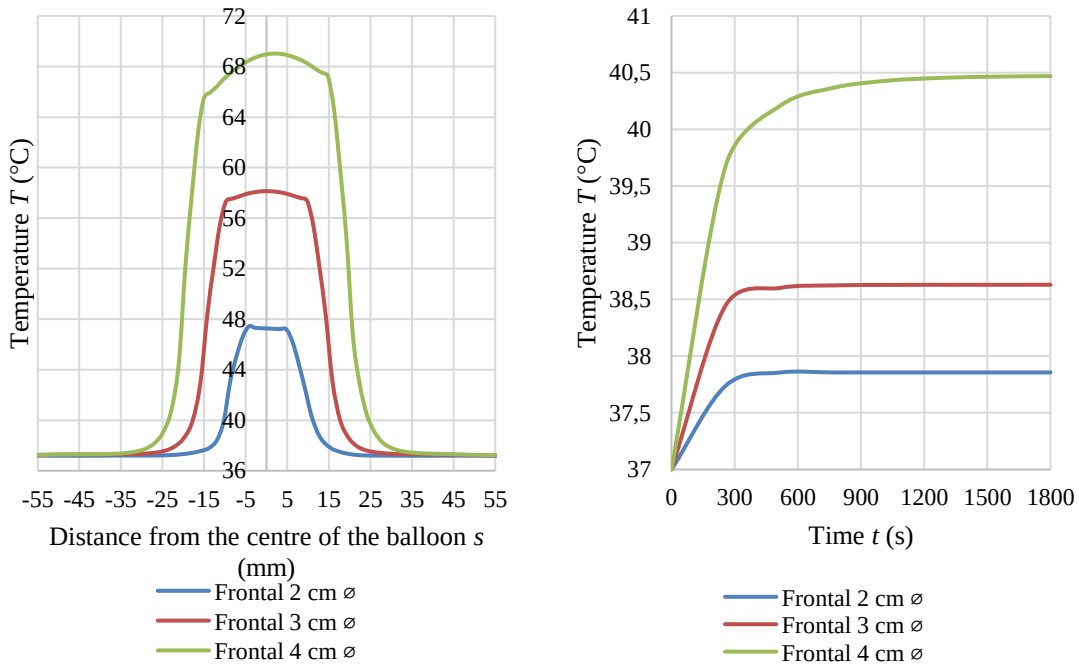

Figure 5.11: Graphical representation of temperature distribution in the 2-coat TBT balloons and in its vicinity (*left*) and the temperature progression throughout the simulation 5 mm from the balloons (*right*) located in frontal lobe of patient model

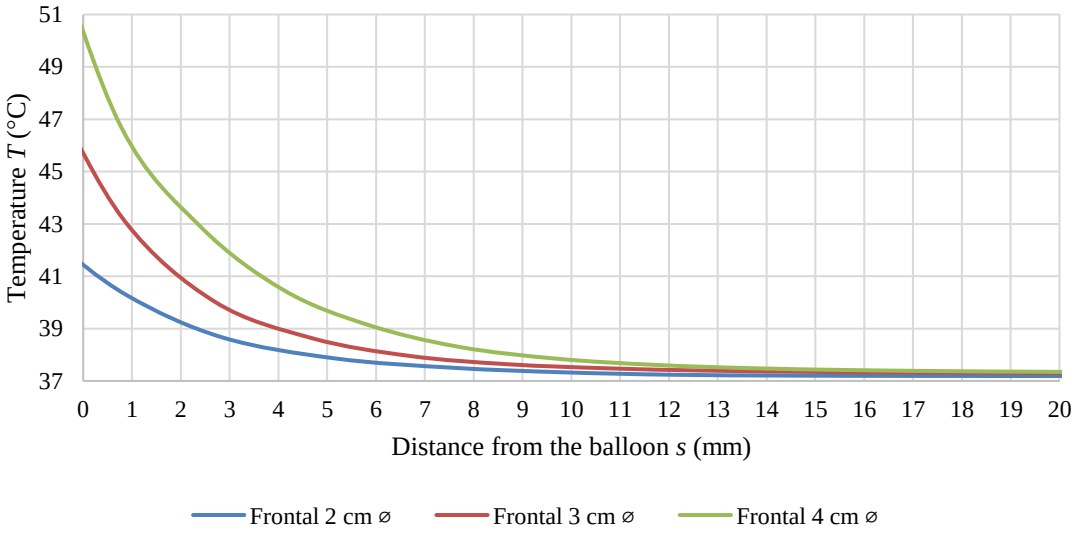

Figure 5.12: Distribution of temperature from the TBT balloons located in the frontal lobe of the patient model

5.2.2 Temporal Lobe

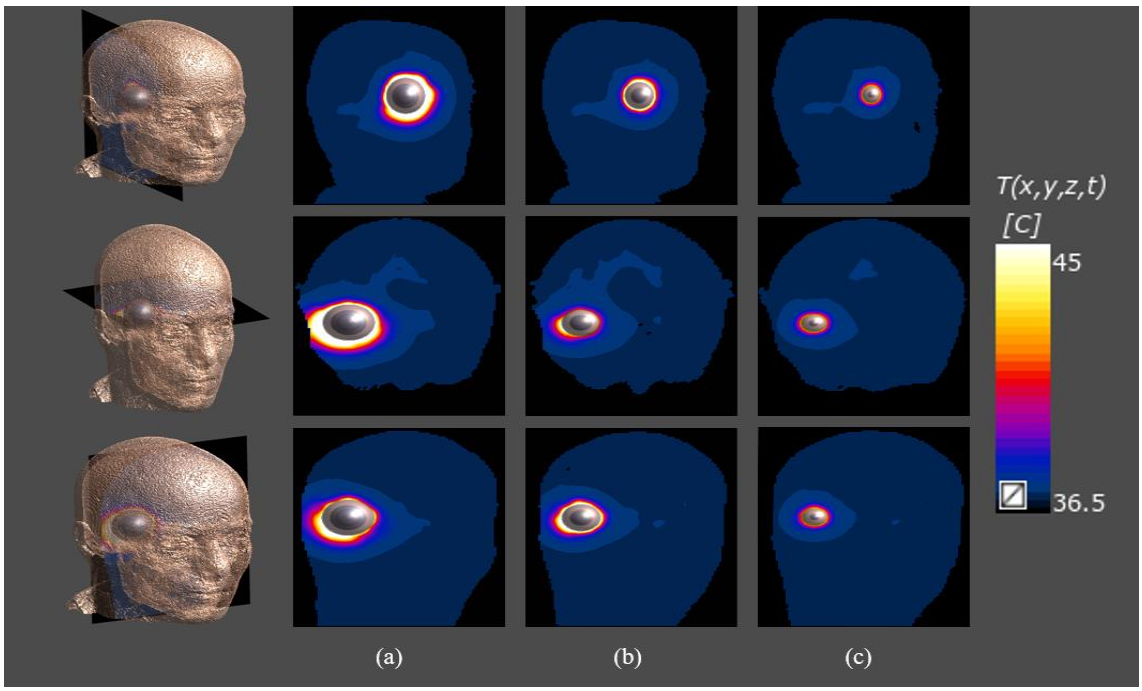

Figure 5.13: Temperature layout around the 2-coat TBT balloons with a 4 (a), 3 (b) and 2 (c) -cm diameter located in a temporal lobe of patient model displayed in sagittal, horizontal and coronal slice, 1800 s after the start of simulation

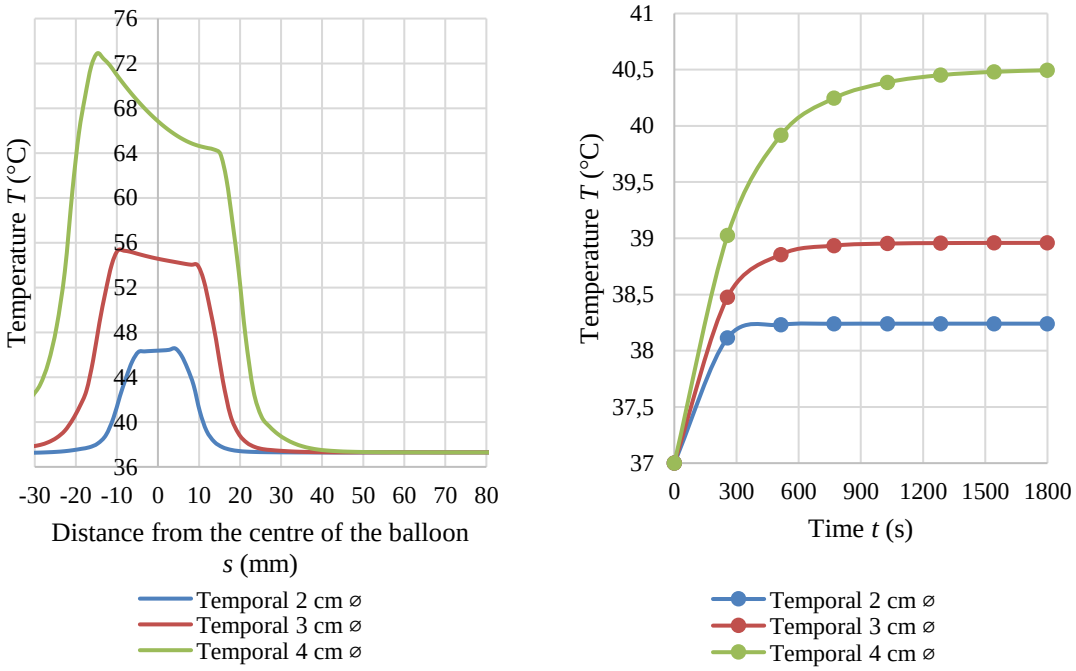

Figure 5.14: Graphical representation of temperature distribution in the 2-coat TBT balloons and in its vicinity (*left*) and the temperature progression throughout the simulation 5 mm from the balloons (*right*) located in temporal lobe of patient model

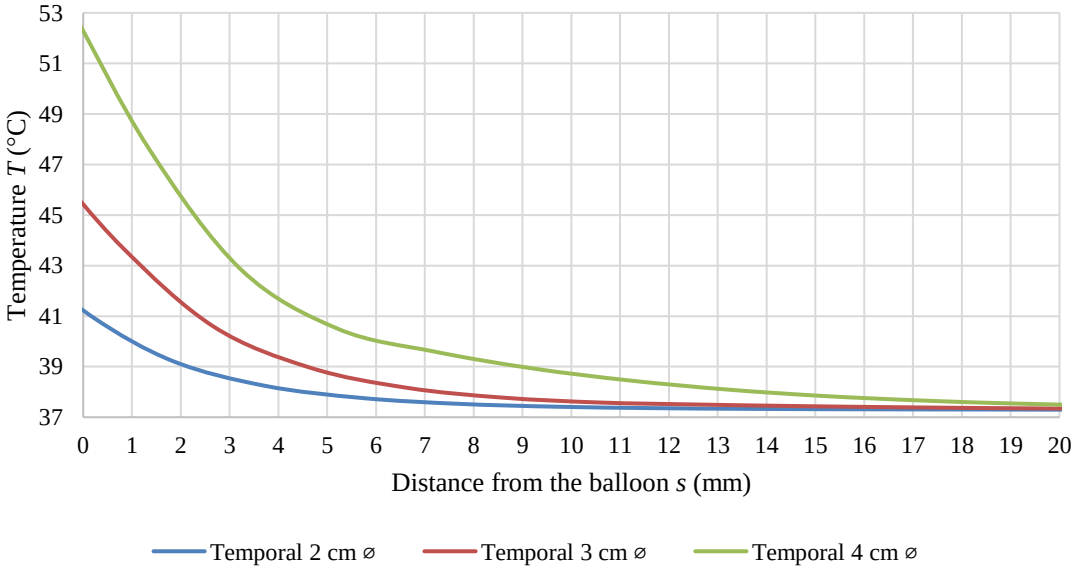

Figure 5.15: Distribution of temperature from the TBT balloons located in the temporal lobe of the patient model

5.2.3 Parietal Lobe

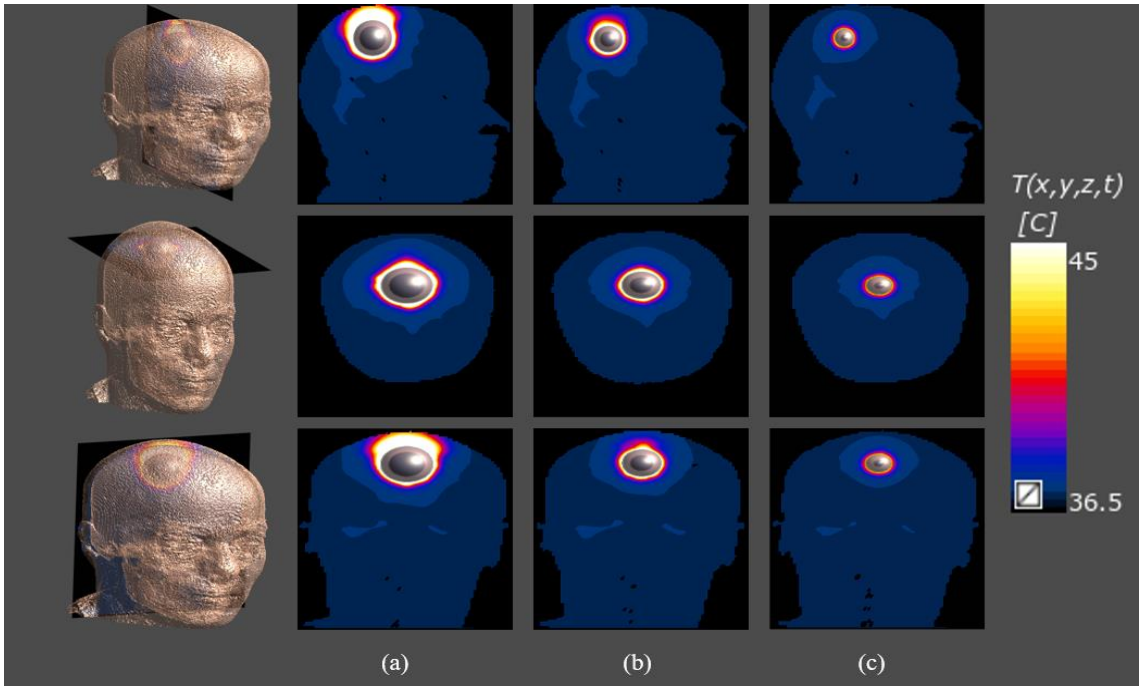

Figure 5.17: Temperature layout around the 2-coat TBT balloons with a 4 (a), 3 (b) and 2 (c) -cm diameter located in a parietal lobe of patient model displayed in sagittal, horizontal and coronal slice, 1800 s after the start of simulation

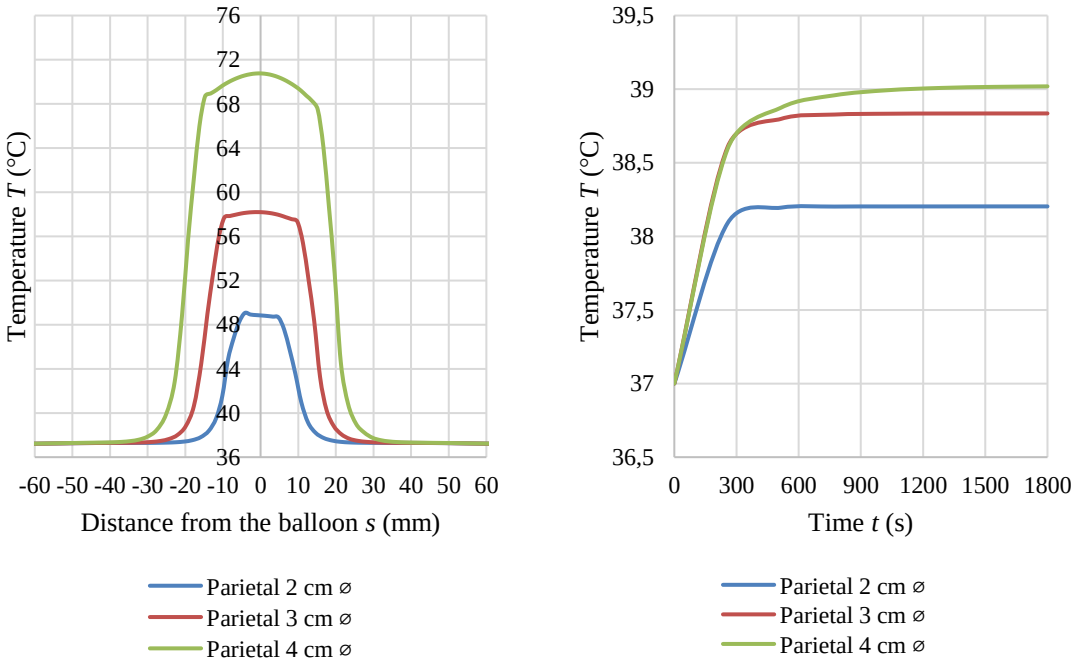

Figure 5.16: Graphical representation of temperature distribution in the 2-coat TBT balloons and in its vicinity (*left*) and the temperature progression throughout the simulation 5 mm from the balloons (*right*) located in parietal lobe of patient model

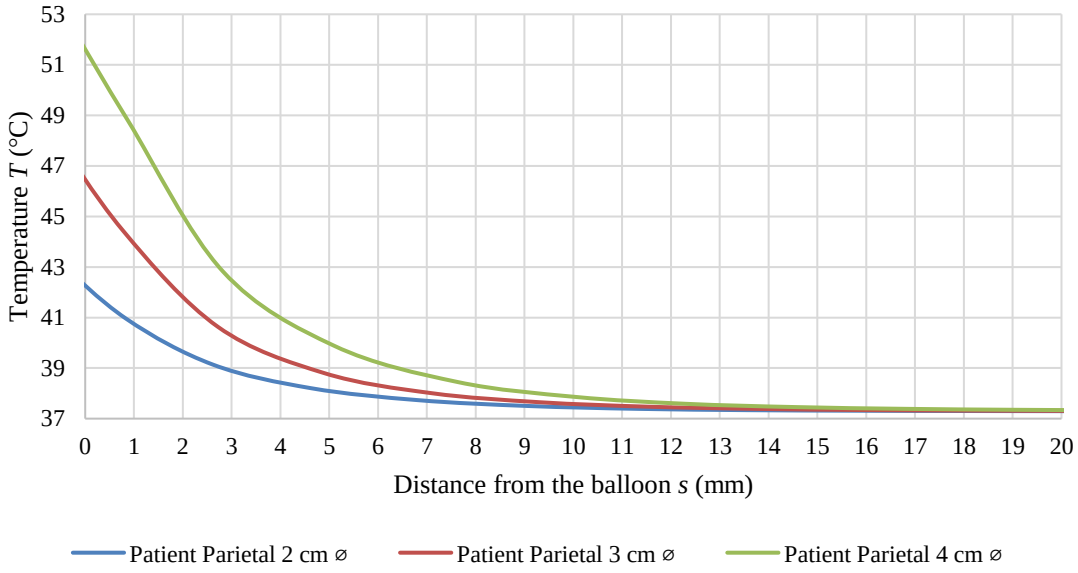

Figure 5.18: Distribution of temperature from the TBT balloons located in the parietal lobe of the patient model

In each lobe of the patient model, the TBT balloon of the diameter 4 cm produced heat which resulted in the temperature higher than 48 °C in the tissue surrounding the resection cavity. Times of this overstep are listed in the table below.

Table 6: Times at which the temperature on the surface of the 2coat balloon reached 48 °C

Location of the balloon	Frontal lobe (⌀ = 4 cm)	Temporal lobe (⌀ = 4 cm)	Parietal lobe (⌀ = 4 cm)
Time *t* (min)	3.5	4.0	3.5

To summarise the results of the heating from double-silicone layered TBT balloons, I created a table, in which I highlighted both excessive and healing temperature ranges. Values in red cells represent the case in which the temperature passed the required limit, green cells contain successfully heated areas. Values in white cells are below the temperature limit and do not meet the hyperthermic conditions.

Table 7: Temperature range in the 5 mm annular rim of tissue surrounding the 2coat TBT balloons

	2-coat models					
	MIDA			***Patient***		
	Temperature range in 5 mm of treated tissue (°C)			Temperature range in 5 mm of treated tissue (°C)		
Lobe	4 cm TBT	3 cm TBT	2 cm TBT	4 cm TBT	3 cm TBT	2 cm TBT
Frontal	38.5–48.5	38.5–46	38–42.5	40–50	39–46	38–41.5
Temporal	39.5–51	40–47	38–42	40.5–52	39–45.5	38–41.5
Parietal	38.5–45.5	38.5–44.5	38–41.5	40–51.5	39–46	38–42

5.3 Models with single-coat TBT balloons

Other simulations were computed for models with a single coat TBT balloons using the values calculated in *Table 1*. In this chapter I present the graphical evaluation of heating from the balloons in parietal lobes. Frontal and temporal lobes were evaluated as well, and their graphical interpretations are part of Attachments A and B.

5.3.1 MIDA

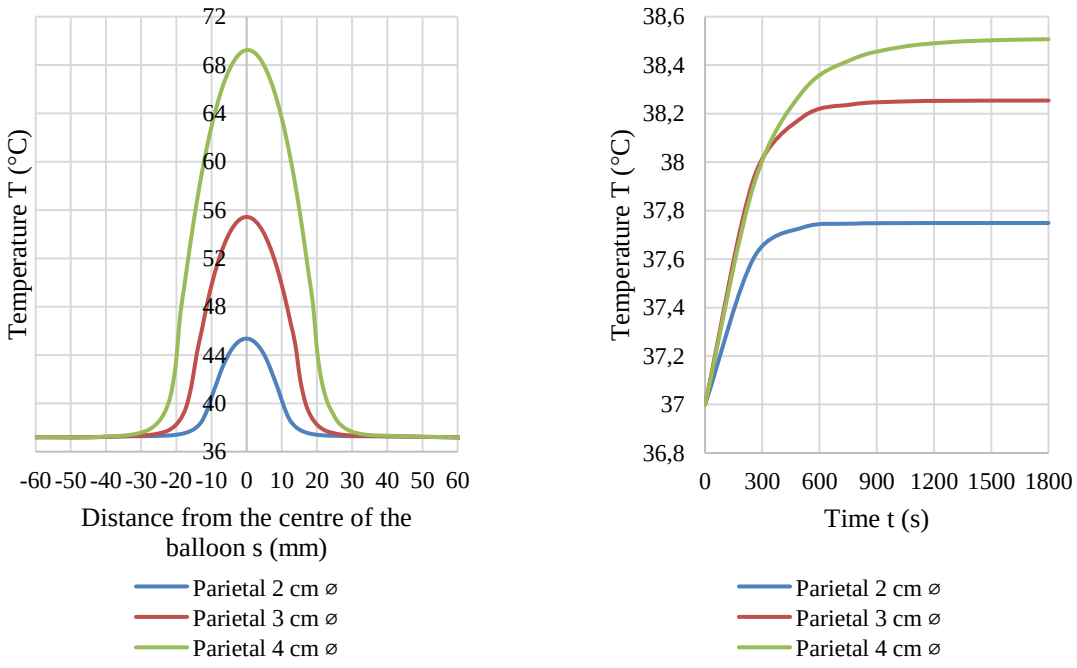

Figure 5.19: Graphical representation of temperature distribution in the 1-coat TBT balloons and in its vicinity (*left*) and the temperature progression throughout the simulation 5 mm from the balloons (*right*) located in parietal lobe of MIDA model

The temperature limit was exceeded only with the TBT balloon in the temporal lobe.

Table 8: Times at which the temperature on the surface of the 1coat balloon reached 48 °C

Location of the balloon	Temporal lobe (⌀ = 4 cm)
Time *t* (min)	6.5

5.3.2 Patient

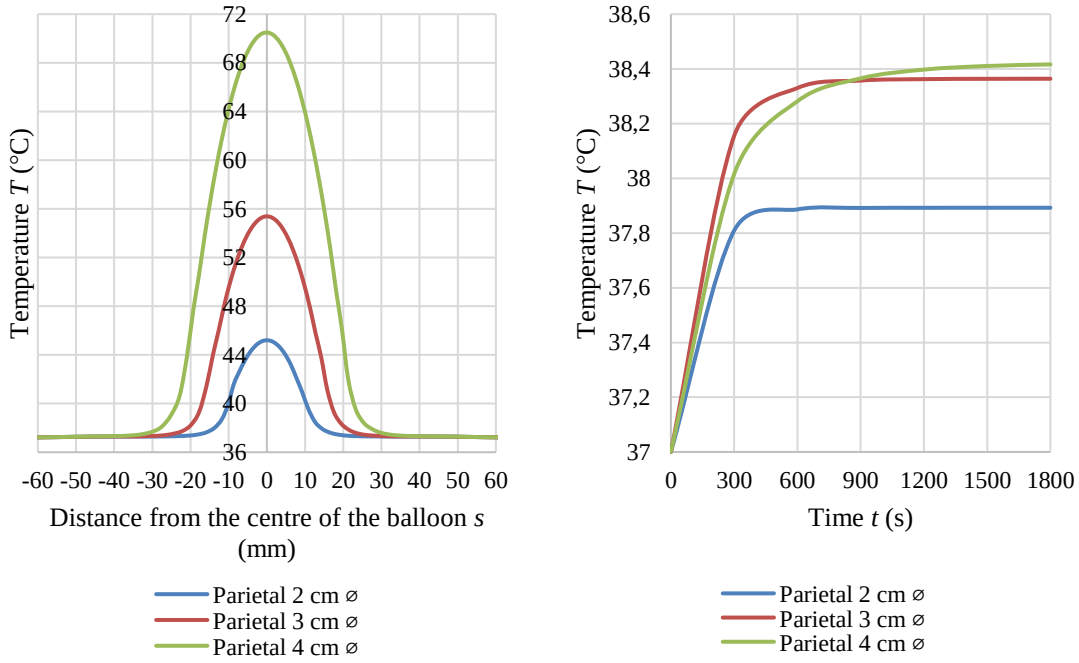

Figure 5.20: Graphical representation of temperature distribution in the 1-coat TBT balloons and in its vicinity (*left*) and the temperature progression throughout the simulation 5 mm from the balloons (*right*) located in parietal lobe of patient model

Similarly, the temperature which would cause ablation in tissue was reached only in the presence of TBT balloon set in the temporal lobe.

Table 9: Times at which the temperature on the surface of the 1coat balloon reached 48 °C

Location of the balloon	Temporal lobe (⌀ = 4 cm)
Time *t* (min)	6.25

To summarise the results of the heating from single-silicone layered TBT balloons, in *Table 10* I state the temperature ranges reached in 5 mm of annular rim of tissue around resection cavity. Values in red cells represent the case in which the temperature passed the required limit while green cells contain successfully heated areas. Values in non-coloured cells are below the temperature limit and do not meet the hyperthermic conditions. 5 – 6

Table 10: Temperature range in the 5 mm annular rim of tissue surrounding the 1coat TBT balloons

	1-coat models					
	MIDA			***Patient***		
	Temperature range in 5 mm of treated tissue (°C)			Temperature range in 5 mm of treated tissue (°C)		
Lobe	4 cm TBT	3 cm TBT	2 cm TBT	4 cm TBT	3 cm TBT	2 cm TBT
Frontal	38.5–44	38.5–43	38.5–42	39–47	38.5–43	38.5–41
Temporal	45–58	38.5–44	38–41.5	46.5–58.5	40–45.5	38–41
Parietal	39.5–44.5	38.5–42	37.5–40	38.5–45.5	38.5–42.5	38–40

5.4 Patient model, hyperperfused, heated constantly at temperature 45 °C

Part of the assignment is to heat the surrounding tissue using a single silicone balloon filled with fluid at temperature from 40 °C to 50 °C. This heating does not require the nanoparticle solution as it is not heated by an electromagnetic coil but the water inside it is set to unchanging temperature value from the mentioned range. However, the results of these simulations were rather monotonous since there was no difference in heating of the individual sizes of the balloons. *Figure 5.21* shows the temperature layout of 3 cranial slices for the balloon of diameter with 4 cm heated to 45 °C, located in the temporal lobe. *Figure 5.22* and *5.23* represents the overall temperature distribution from the silicone of three sizes of the balloons located in parietal and temporal lobes.

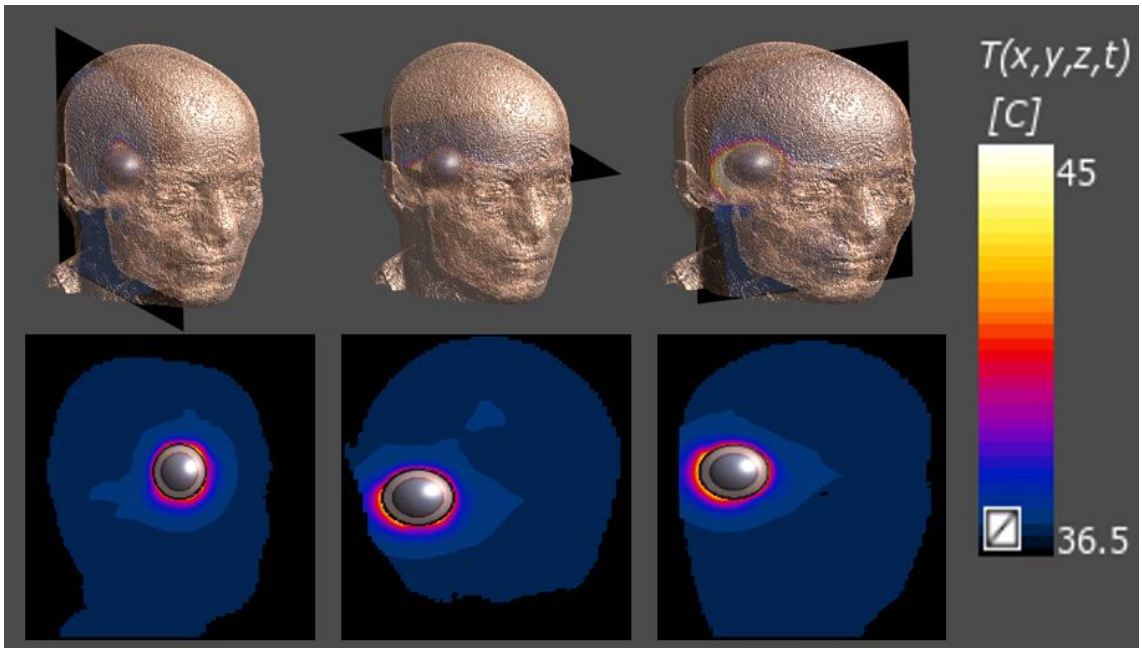

Figure 5.22: Temperature layout around the balloon with diameter 4 cm, heated constantly at 45 °C, located in temporal lobe of patient model, illustrated in sagittal, horizontal and coronal slices, 1800 s after the start of simulation

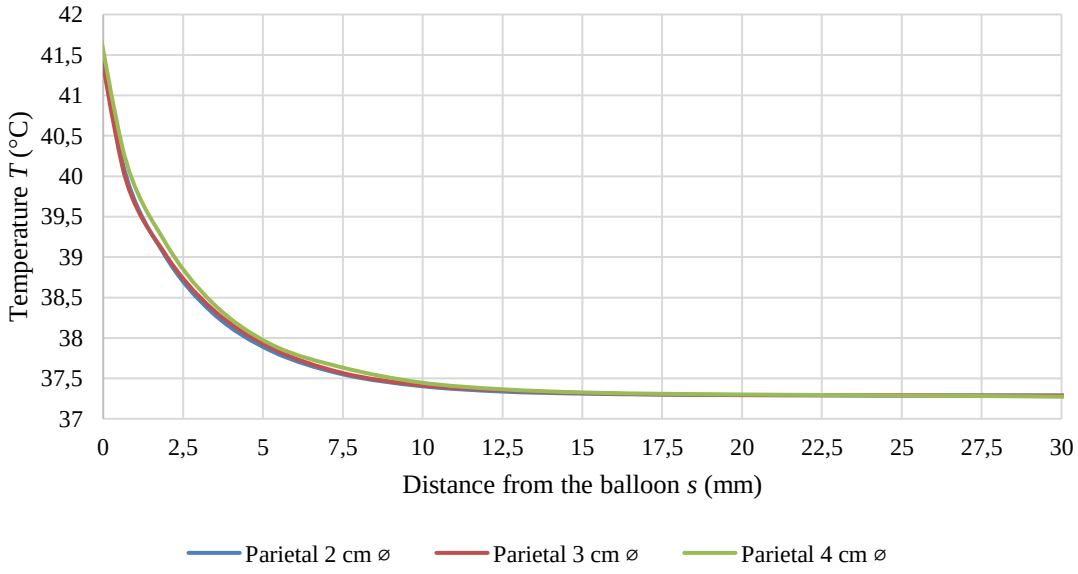

Figure 5.21: Distribution of temperature from the TBT balloons located in the parietal lobe of patient model heated constantly at 45 °C

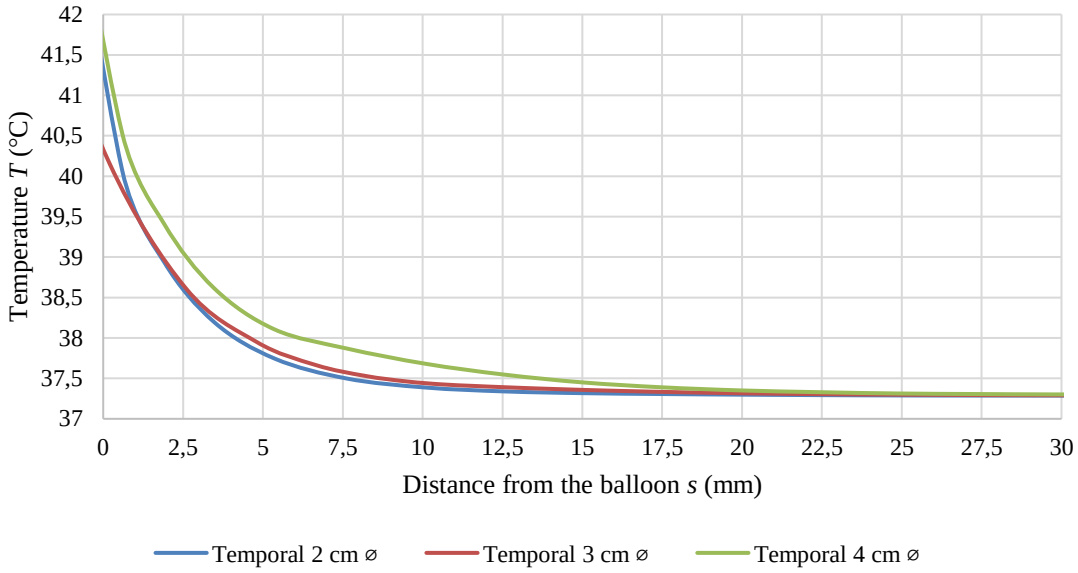

Figure 5.23: Distribution of temperature from the TBT balloons located in the temporal lobe of patient model heated constantly at 45 °C

5.5 Comparison of MIDA model and Patient model

As the position of TBT balloons in both models is alike, it is possible to compare how the temperature progressed in the surrounding tissue of resection cavities. This comparison shows the impact of multiple tissues of different densities and thermal properties on the overall temperature distribution around the TBT balloons. In MIDA model, not only white matter surrounded the balloons, but vessels, nerves, and meninges as well. *Figure 5.24* examines the difference in how the tissues around the outer layer of the TBT balloons in parietal lobe were heated for MIDA model and patient model. Results for frontal and temporal lobes are corresponding.

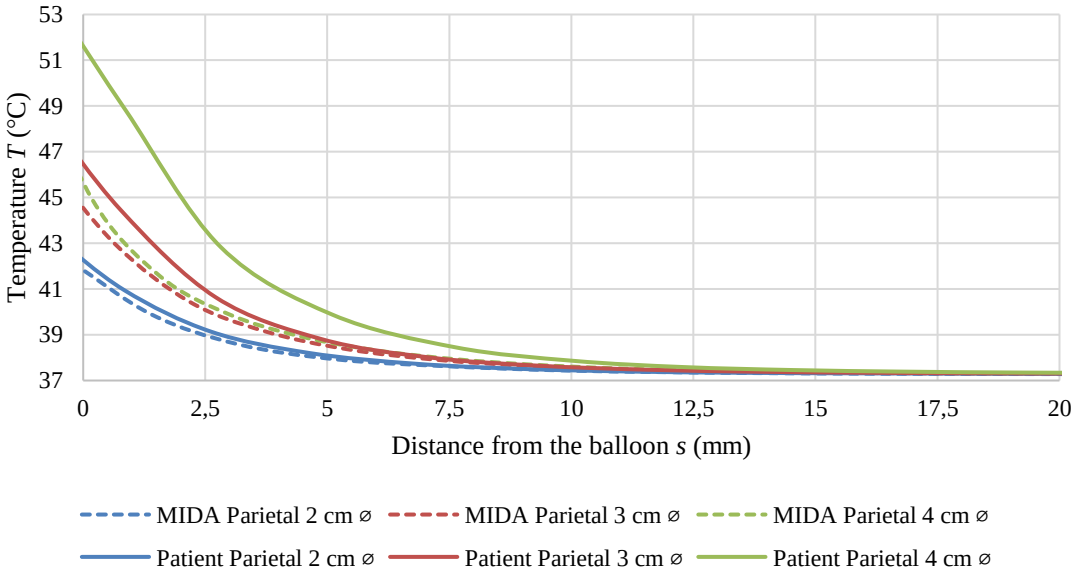

Figure 5.24: Distribution of temperature from the TBT balloons considering the differences between MIDA model and patient model

5.6 Comparison of 1-coat and 2-coat MIDA model

To compare two heating models of single and double layered TBT balloon, following graph was constructed. These heating models differ in the value of heat generation rate calculated from *Tables 1* and *2*. For illustration, the heating system in the frontal lobes of hyper-perfused MIDA models was used. The results in the two other lobes were equivalent with the only difference in maximal temperature reached in temporal lobe. The double-coat balloon with diameter 4 cm, located in temporal lobe, produced excessive heating which resulted in the temperature of almost 53 °C on the right side and more than 55 °C on the left side of the outer balloon 's surface.

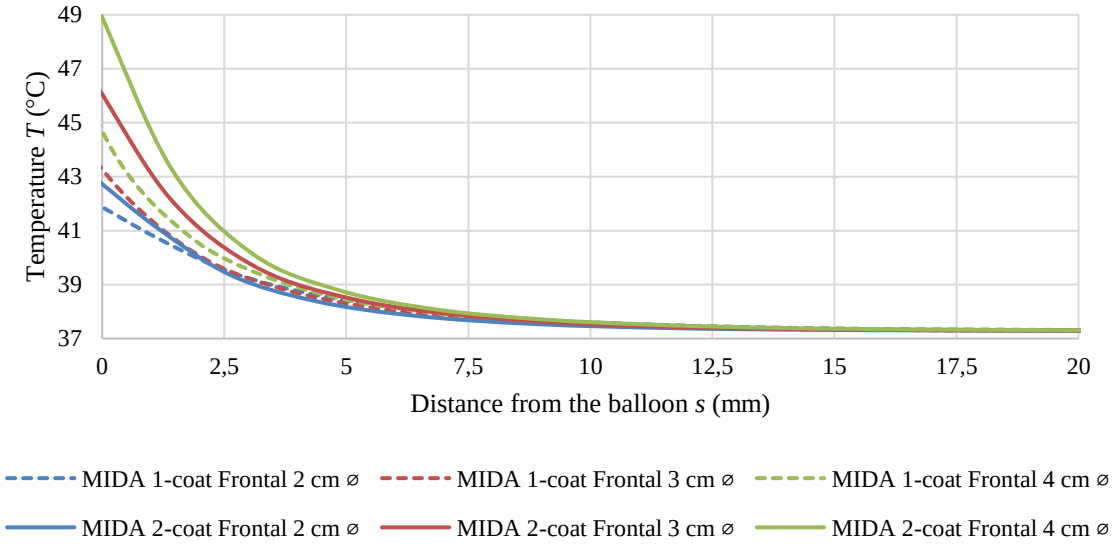

Figure 5.25: Distribution of temperature from the TBT balloons considering the differences between 1-coat and 2-coat TBT heating balloon

5.7 Comparison of normo-perfused and hyper-perfused MIDA model

Following graph shows the differences in the heating extent of the hyper-perfused model and normo-perfused model of MIDA. The comparison of patient models was not

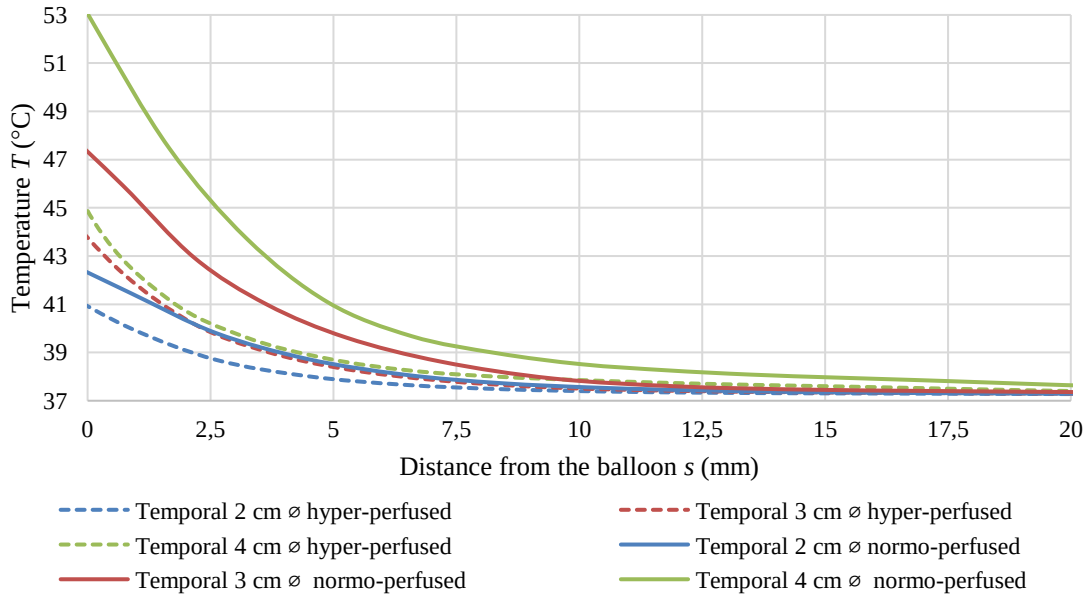

Figure 5.26: Distribution of temperature from the TBT balloons considering the differences between hyper-perfused and normo-perfused MIDA model

chosen, as the only change was in the perfusion of white matter since the model does not contain muscle and fat tissues. It compares the temperature distributions from 1-coat TBT balloons located in temporal lobes. The results for parietal and frontal lobes are corresponding. differing only in the temperature maxima. The graph represents the state at the end of the simulation, that means after thirty minutes of heating.

5.8 Comparison of nano-heated TBT balloon and balloon heated constantly at temperature 45 °C

It is necessary to provide the distinction of the balloon heated by nanoparticles with different intensities of magnetic field and the balloon heated solely by hot fluid set to constant temperature. As was mentioned in *Chapter 5.4* the later heating model presented unambiguous results without differences between the sizes of the balloons. Following comparison shows that the nanoparticles-heated system provides more intense heating with distinctions for the size of the balloon.

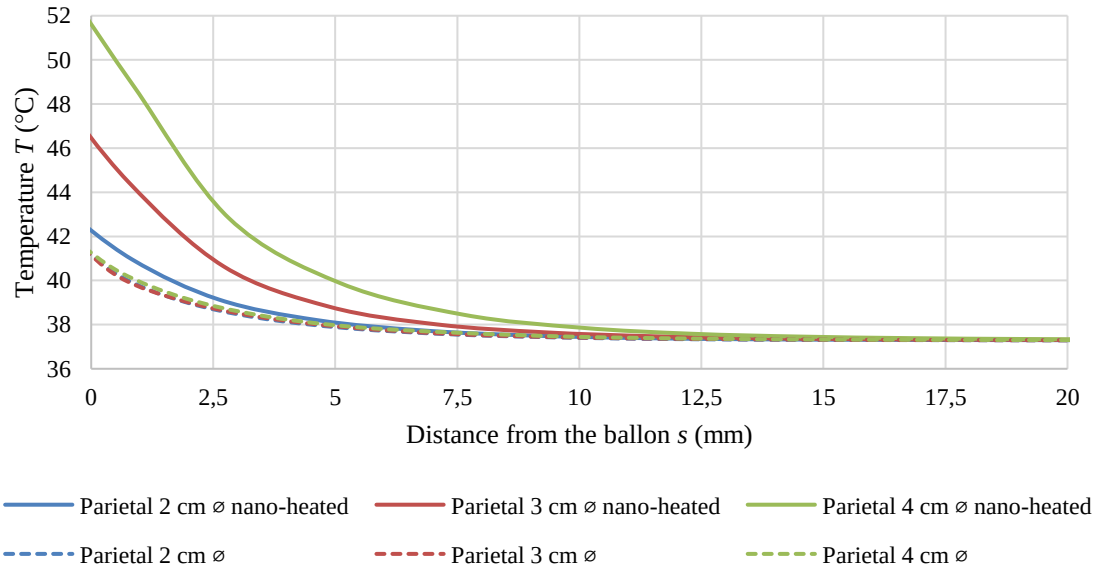

Figure 5.27: Distribution of temperature from the TBT balloons considering the differences between TBT-balloons heated by nanoparticles and by the fluid set constantly to 45 °C

5.9 Impact of veins and arteries

The positions of TBT balloons in the MIDA model were in the proximity of main veins and arteries. As the blood vessels have different thermal properties and perfusion rates, there is a change in the overall temperature increase from the source of heating. The graphs below depict the influence of veins and arteries. In *Figure 5.29*, the Superior sagittal sinus of Internal jugular vein is at the position -20 mm from the zero point and in *Figure 5.30* the Superficial temporal artery is at the position -15 mm from the zero point.

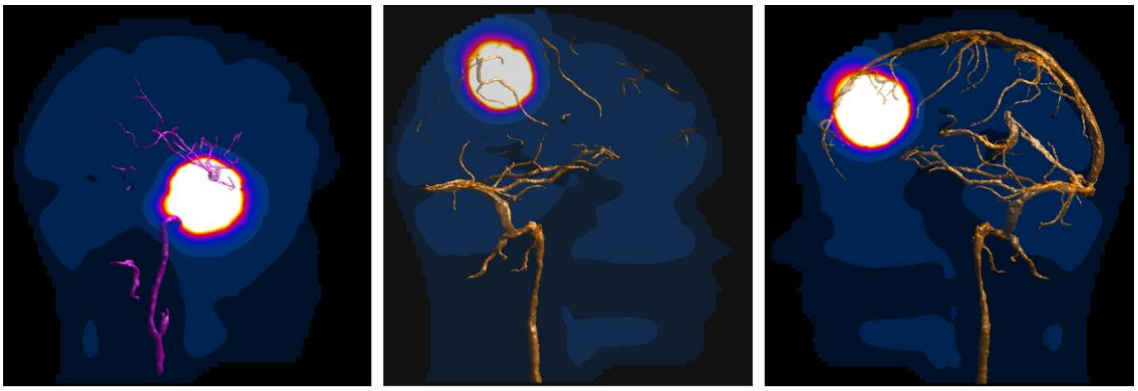

Figure 5.28: Location and impact of vessels near the TBT balloons of 4cm diameters, located in temporal (a), parietal (b) and frontal (c) lobe viewed in sagittal section

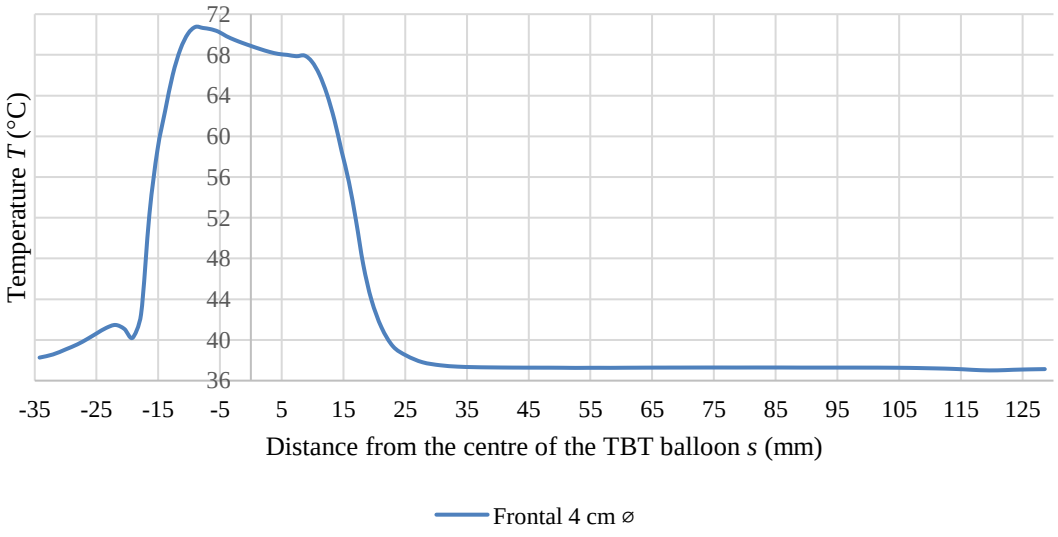

Figure 5.29: The temperature outline in the vicinity of the Internal jugular vein located near the surface of the TBT balloon

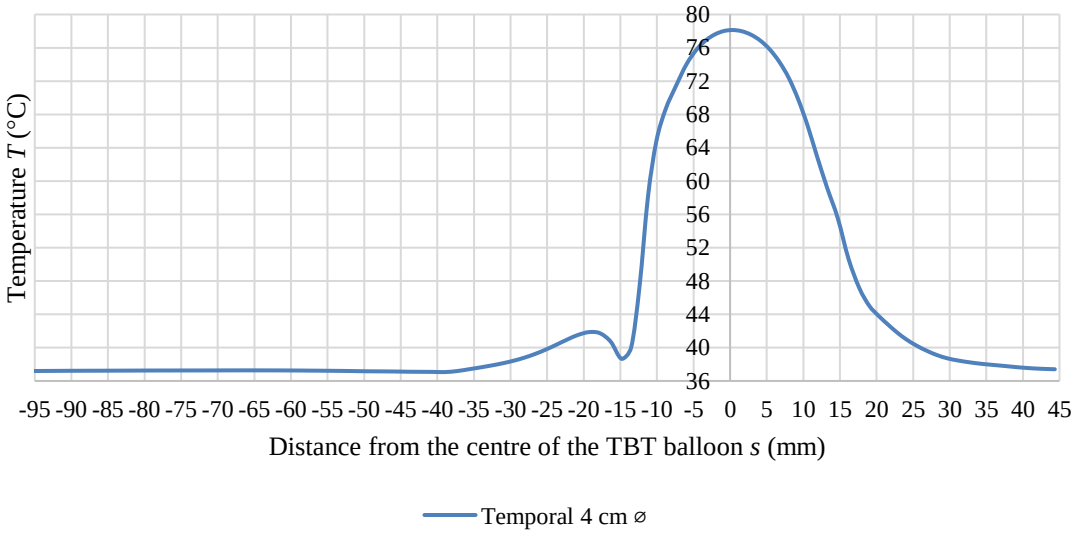

Figure 5.30: The temperature outline in the vicinity of the Superficial temporal artery located near the surface of the TBT balloon

6 Discussion

From the simulation variations that were computed, the results can by analysed according to the ability to heat the 5mm tissue rim that surrounds the resection cavity /in our case the balloon) to the temperature from 39 °C to 48 C. The temperatures below this level would not induce more effective radiotherapy and temperatures above 48 °C would cause unwanted ablation to the tissue resulting in its necrosis.

The results of the simulation from 2-coat TBT balloon show that the desired temperature range for the 5 mm of tissue is reached only around the middle-sized TBT balloons and around a balloon of 4 cm diameter located in the parietal lobe of MIDA model. Rest of the 4 cm balloons are causing excessive heating of the tissue surrounding them. In *Tables 5* and *6* I stated times at which the temperature limit was exceeded. These high temperatures may be avoided by lowering the intensity of the electromagnetic field at the specified times or by reducing the layer of nanoparticle solution. None of the smallest balloons with diameter of 2 cm was able to heat the 5 mm of annular rim of tissue around them. These balloons were capable of delivering the required value of heat only to the distance of 2 to 3 mm.

Single-coated models met the conditions in more cases than balloons in the previous set of simulations. The therapeutic amplitudes were reached around all 3cm TBT balloons as well as in the 2-coat models. Furthermore, two larger sizes of balloons in parietal and temporal lobes delivered the prescribed heat to the tissues of both models. The temperature limit was topped around the largest balloons in temporal lobes around the 6^{th} minute of simulations.

From the obtained results it can be concluded that the smallest size of the balloon (with 2cm diameter) is not capable of heating the tissue to the extent of 5 mm from its silicone coating. This size is not recommended for the use of thermobrachytherapy. Furthermore, use of the biggest size of the balloon usually results in an excessive heating. As this size was capable of heating even the tissues 5 mm from the balloon in the majority of cases, it is recommended to adjust the field intensity of coil or to chose thinner layer of nanofluid in 2-coat models rather than not using it at all. The golden middle way was reached with the balloons of 3cm diameter as it showed the capability of heating the tissue to the least extreme extent. The figures of model slices show that the heating was

disproportionated on the sides were the balloons neighboured with meninges of the brain where the temperature was vastly dissipated.

Temperature of each model stabilises between the sixth and the eighth minute and from this point behaves constantly.

From the comparison of chosen modalities there are following results:

1. Heating of cranial model of patient showed more intense heating than the model of MIDA. (*Figure 5.24*)

This is probably due to the uniformity in the surroundings of resection cavities in patient model, as no other tissues than white matter, alternatively gray matter were considered. On the other hand, in MIDA model, there were several tissues with higher perfusion rates that may have reduced the temperature layout. These tissues include blood arteries and veins, as well as CSF or meninges of brain.

2. Double-layered TBT balloons produced more heating than the single-layered ones. (*Figure 5.25*)

This is because of the obvious fact that power produced by the 2-coat TBT balloons is higher than in the 1-coat balloons. Values of power loss were obtained from the bachelor thesis "*Inductive heating of magnetic nanoparticles for hyperthermia*" [29] and they are listed in *Tables 1* and *2*.

3. Heating of normo-perfused model was more profound than the heating of hyper-perfused model. (*Figure 5.26*)

Accelerated blood flow is responsible for better circulation, therefore the heated blood is frequently carried out from the tissue. This is part of the cooling mechanism of the brain. The results obtained from the hyper-perfused models show the real response of the healthy brain to the hyperthermia.

4. Balloons filled with nanoparticles provide deeper heating than the ones filled with fluids set to constant hyperthermic temperatures. (*Figure 5.27*)

This statement proves that nanoparticle heating is the optimate method used for thermobrachytherapy.

Position of veins near the balloon affects the temperature distribution in the vicinity of balloon. This is shown in *Figures 5.29* and *5.30* by a visible drop of more than 2 °C.

This decline is the result of high perfusion rate of vessels, which is more than twenty times higher than the perfusion of the white matter.

The inaccuracies in the results of temperature distribution in tissues may have been caused by coarse voxeling of models during simulations where the temperature values on the edges of materials are approximated to the values behind their boundaries.

The most challenging demand of this thesis was the implementation of the perfusion values at hyperthermic conditions. The studies dealing with this subject were mostly out-of-date and did not carry out the values for brain structures. I suggest more research on this topic as the results of simulations may be distorted since the actual physiological processes in the brain during hyperthermia are not properly captured. Another advance to this study would be the calculation of the radiation dose needed to be delivered to the tissue with hyperthermia lowering the required ionisation energy.

7 Conclusion

This study dealt with the treatment technique of thermobrachytherapy used for prolonging the lifespan of patients with glioblastomas by proper elimination of possible metastatic residues left after the resection surgery. I studied the thermal approach of this method by simulating the heating of tissues around the resection cavity from the thermobrachytherapy balloon.

The simulations were performed on two head models. The first one, MIDA model [27] was detailed cranial model composed of 117 structures, the other model was simplified design of patient model made up of 6 main materials. Results show that the heating was more profound in less-detailed patient model. The graphical representations of the simulation results of the heating from double-layered thermobrachytherapy balloons are part of *Chapter 5.1* and *5.2*. For the simulations of heating the same head models from the simplified 1-coat TBT balloon, results are displayed in *Chapter 5.3* and in the Attachments A & B. I compared all the simulations in the set of graphs, as part of the chapter *Results*. The comparisons confirmed that the hyper-perfusion of tissues results in less profound heating. Heating from the balloons filled with nanoparticle solution has proven to be more effective than the suggested method of heating from the balloons filled with hot water.

From the obtained results, I conclude that the thermobrachytherapy treatment is effective for the balloons with diameters of 3 cm and the region of brain that is the most suitable for this treatment technique is the parietal lobe.

References

[1] KREX, D., B. KLINK, C. HARTMANN et al. Long-term survival with glioblastoma multiforme. Brain [online]. 2007, 130(10), 2596-2606. DOI: 10.1093/brain/awm204. ISSN 0006-8950. Available on*: https://academic*.oup.com/brain/article-lookup/doi/10.1093/brain/awm204

[2] HOLLAND, E. C. Glioblastoma multiforme: The terminator. Proceedings of the National Academy of Sciences [online]. 2000, 97(12), 6242-6244. *DOI:* 10.1073/pnas.97.12.6242. ISSN 0027-8424. Available on: http://www.pnas.org/cgi/doi/10.1073/pnas.97.12.6242

[3] HANIF, Farina, Kanza MUZAFFAR a Kahkasaan PERVEEN. Glioblastoma Multiforme: A Review of its Epidemiology and Pathogenesis through Clinical Presentation and Treatment. Asian Pacific Journal of Cancer Prevention *[online]. 2017, 18(1), 3-9*. DOI: 10.22034/APJCP.2017.18.1.3. Available on: https://www.ncbi.nlm.nih.gov/pmc/articles/PMC5563115/

[4] STAUFFER, Paul, Dario RODRIGUES, Robert GOLDSTEIN et al. Dual Modality Implant for Simultaneous Magnetic Nanoparticle Heating and Brachytherapy Treatment of Tumor Resection Cavities *in Brain*. In: 2018 IEEE/MTT-S International Microwave Symposium - IMS [online]. Philadelphia, PA, USA: IEEE, 2018, s. 1285-1287. DOI: 10.1109/MWSYM.2018.8439348. ISBN 978-1-5386-5067-7. Available on: https://ieeexplore.ieee.org/document/8439348/

[5] LANG, J., B. ERDMANN a B. SEEBASS. Impact of nonlinear heat transfer on temperature control in regional hyperthermia. IEEE Transaction on Biomedical *Engineering.* IEEE Transaction on Biomedical Engineering. 1999, 46(9), 1129-1138.

[6] HENDRIX, Philipp, Elisa HANS, Christoph GRIESSENAUER, Andreas SIMGEN, Joachim OERTEL a Julia KARBACH. Neurocognitive status in patients with newly-diagnosed brain tumors in *good* neurological condition: The impact of tumor type, volume, and location. Clinical Neurology and

Neurosurgery [online]. 2017, 156, 55-62. DOI: 10.1016/j.clineuro.2017.03.009. ISSN 03038467. Available on: https://linkinghub.elsevier.com/retrieve/pii/S0303846717300768

[7] DAVIS, Mary. Glioblastoma: Overview of Disease and Treatment. Clinical Journal of Oncology Nursing [online]. 2016, 20(5), 2-8. DOI: 10.1188/16.CJON.S1.2-8. ISSN 1092-1095. Available on: http://cjon.ons.org/cjon/20/5/supplement/glioblastoma-overview-disease-and-treatment

[8] NAVRÁTIL, Leoš a Jozef ROSINA. Medicínská biofyzika. 2., zcela přepracované a doplněné vydání. Praha: Grada Publishing, 2019. ISBN 978-80-271-0209-9.

[9] KREX, Dietmar, Barbara KLINK a Christian HARTMANN. Long-term survival with glioblastoma multiforme. Brain. 2007, 130(10), 2596-2606.

[10] LOUIS, David, Hiroko OHGAKI, Otmar WIESTLER, Webster CAVENEE, Peter BURGER, Anne JOUVET, Bernd SCHEITHAUER a Paul KLEIHUES. The 2007 WHO Classification *of Tumours* of the Central Nervous System. Acta Neuropathologica [online]. 2007, 114(2), 97-109. DOI: 10.1007/s00401-007-0243-4. ISSN 0001-6322. Available on: http://link.springer.com/10.1007/s00401-007-0243-4

[11] NELSON, Sarah a Soonmee CHA. Imaging Glioblastoma Multiforme. The Cancer Journal [online]. 2003, 9(2), 134-145. DOI: *10.*1097/00130404-200303000-00009. ISSN 1528-9117. Available on: http://journals.lww.com/00130404-200303000-00009

[12] LARJAVAARA, Suvi, Riitta MÄNTYLÄ, Tiina SALMINEN, Hannu HAAPASALO, Jani RAITANEN, Juha JÄÄSKELÄINEN a Anssi AUVINEN. Incidence of gliomas by anatomic location. Neuro-Oncology [online*]. 2007, 9(3),* 319-325. DOI: 10.1215/15228517-2007-016. ISSN 1523-5866. Available on: http://academic.oup.com/neuro-oncology/article/9/3/319/1051058/Incidence-of-gliomas-by-anatomic-location

[13] MANN, Justin, Rohan RAMAKRISHNA, Rajiv MAGGE a A. WERNICKE. Advances in Radiotherapy for Glioblastoma. Frontiers in Neurology [online]. 2018, 8. *DOI: 10.3389*/fneur.2017.00748. ISSN 1664-2295. Available on: http://journal.frontiersin.org/article/10.3389/fneur.2017.00748/full

[14] LEE, Sang. Temozolomide resistance in glioblastoma multiforme. Genes & Diseases [online]. 2016, 3(3), 198-210. DOI: 10.*1016/*j.gendis.2016.04.007. ISSN 23523042. Available on: https://linkinghub.elsevier.com/retrieve/pii/S2352304216300162

[15] SONG, C, M KANG, J RHEE a S LEVITT. The effect of hyperthermia on vascular function, pH, and cell survival. Radiology [*online]*. 1980, 137(3), 795-803. DOI: 10.1148/radiology.137.3.7444064. ISSN 0033-8419. Available on: http://pubs.rsna.org/doi/10.1148/radiology.137.3.7444064

[16] BARONZIO, Gian a E. HAGER. Hyperthermia in cancer treatment: a primer. New York, N.Y.: Springer Science + Business Media, 2006. ISBN 978-0387334400.

[17] MAIER-HAUFF, Klaus, Frank ULRICH, Dirk NESTLER et al. Efficacy and safety of intratumoral thermotherapy using magnetic iron-oxide nanoparticles combined with external beam radiotherapy *on patients* with recurrent glioblastoma multiforme. Journal of Neuro-Oncology [online]. 2011, 103(2), 317-324 [cit. 2020-05-13]. DOI: 10.1007/s11060-010-0389-0. ISSN 0167-594X. Available on: http://link.springer.com/10.1007/s11060-010-0389-0

[18] BLOWERS, Stephen, Ian MARSHALL, Michael THRIPPLETON, Peter ANDREWS, Bridget HARRIS, Iain BETHUNE a Prashant VALLURI. How does blood regulate cerebral temperatures during *hypothermia?*. Scientific Reports [online]. 2018, 8(1). DOI: 10.1038/s41598-018-26063-7. ISSN 2045-2322. Available on: http://www.nature.com/articles/s41598-018-26063-7

[19] MILLIGAN, A.J., P.B. CONRAN, M.A. ROPAR, H.A. MCCULLOCH, R.K. AHUJA a R.R. DOBELBOWER. Predictions of blood flow from thermal clearance during regional hyperthermia. *International Journal of Radiation*

*Oncology*Biology*Physics* [online]. 1983, 9(9), 1335-1343. DOI: 10.1016/0360-3016(83)90265-1. ISSN 03603016. Available on: https://linkinghub.elsevier.com/retrieve/pii/0360301683902651

[20] BUSIJA, D., C. LEFFLER a M. POURCYROUS. Hyperthermia increases cerebral metabolic rate and blood flow in neonatal pigs. American Journal of Physiology-Heart *and* Circulatory Physiology [online]. 1988, 255(2), 343-346. DOI: 10.1152/ajpheart.1988.255.2.H343. ISSN 0363-6135. Available on: https://www.physiology.org/doi/10.1152/ajpheart.1988.255.2.H343

[21] MORIYAMA, Eiji. Cerebral Blood Flow Changes During Localized Hypertherm. Neuro Med Chir (Tokyo). 1990, (30), 923-929.

[22] MCTYRE, Emory, Jacob SCOTT a Prakash CHINNAIYAN. Whole brain radiotherapy for brain metastasis. Surgical Neurology International [online]. 2013, 4(5). DOI: 10.4103/2152-7806.111301. ISSN 2152-7806. Available on: http://surgicalneurologyint.com/surgicalint-articles/whole-brain-radiotherapy-for-brain-metastasis/

[23] KIM, Yeon-Joo, Kwan CHO, Joo-Young KIM et al. Single-Dose Versus Fractionated Stereotactic Radiotherapy for Brain Metastases. International Journal of Radiation Oncology*Biology*Physics *[online*]. 2011, 81(2), 483-489. DOI: 10.1016/j.ijrobp.2010.05.033. ISSN 03603016. Available on: https://linkinghub.elsevier.com/retrieve/pii/S036030161000756X

[24] DALE, R a B JONES. The clinical radiobiology of brachytherapy. The British Journal of Radiology [online]. 1998, 71(845), 465-483. DOI: 10.1259/bjr.71.845.9691890. ISSN 0007-1285. Available on: http://www.birpublications.org/doi/10.1259/bjr.71.845.9691890

[25] MEIGOONI, Ali, Jerome MELI a Ravinder NATH. Interseed effects on dose for 125 I brachytherapy implants. Medical Physics [online]. 1992, 19(2*)*, 385-390. DOI: 10.1118/1.596871. ISSN 00942405. Available on: http://doi.wiley.com/10.1118/1.596871

[26] SUH, John a Gene BARNETT. BRACHYTHERAPY FOR BRAIN TUMOR. *Hematology/Oncology Clinics of North America* [online]. 1999, 13(3), 635-650. DOI: 10.1016/S0889-8588(05)70080-0. ISSN 08898588. Available on: https://linkinghub.elsevier.com/retrieve/pii/S0889858805700800

[27] IACONO, Maria, Esra NEUFELD, Esther AKINNAGBE et al. MIDA: A Multimodal Imaging-Based Detailed Anatomical Model of the Human Head and Neck. *PLOS ONE* [online]. 2015, 10(4), 35. DOI: 10.1371/journal.pone.0124126. ISSN 1932-6203. Available on: https://dx.plos.org/10.1371/journal.pone.0124126

[28] HASGALL, PA, F DI GENNARO, C BAUMGARTNER, E NEUFELD, B LLOYD a MC GOSSELIN. *IT'IS Database for thermal and electromagnetic parameters of biological tissues: Version 4.0* [online]. Available on: https://itis.swiss/virtual-population/tissue-properties/overview/

[29] ADAM, Vojtěch. *Indukční ohřev magnetických nanočástic pro hypertermii*. Praha, 2019.. Bachelor Thesis. České vysoké učení technické v Praze, Fakulta biomedicínského inženýrství. Supervisor: Doc. Ing. David Vrba, Ph.D.

[30] SYAM SUNDAR, L., Manoj SINGH a Antonio SOUSA. Investigation of thermal conductivity and viscosity of Fe3O4 nanofluid for heat transfer applications. *International Communications in Heat and Mass Transfer* [online]. 2013, 44, 7-14. DOI: 10.1016/j.icheatmasstransfer.2013.02.014. ISSN 07351933. Available on: https://linkinghub.elsevier.com/retrieve/pii/S0735193313000420

[31] Overview of materials for Silicone Rubber. *MatWeb, LLC: Material Property Data* [online]. MatWeb, LLC, 2020 Kraft Drive, Suite 3005, Blacksburg, VA 24060., 2018. Available on: http://www.matweb.com/search/datasheet.aspx?matguid=cbe7a469897a47eda563816c86a73520&ckck=1

[32] OZBEK, Husey a Phillips SYDNEY L. *Thermal Conductivity of Aqueous NaCl Solutions from 20°C to 330°C*. Lawrence Berkeley Laboratory University of California Berkeley, CA 94720, 1979.

[33] RIBEIRO, Iva, Netteke VAN HOLTHE, Gerard VAN RHOON a Margarethus PAULIDES. Impact of segmentation detail in hyperthermia treatment planning: comparison between detailed and clinical tissue segmentation. In: *2018 EMF-Med 1st World Conference on Biomedical Applications of Electromagnetic Fields (EMF-Med)* [online]. IEEE, 2018, s. 1-2. DOI: 10.23919/EMF-MED.2018.8526077. ISBN 978-9-5329-0079-8. Available on: https://ieeexplore.ieee.org/document/8526077/

Attachment A: Figures

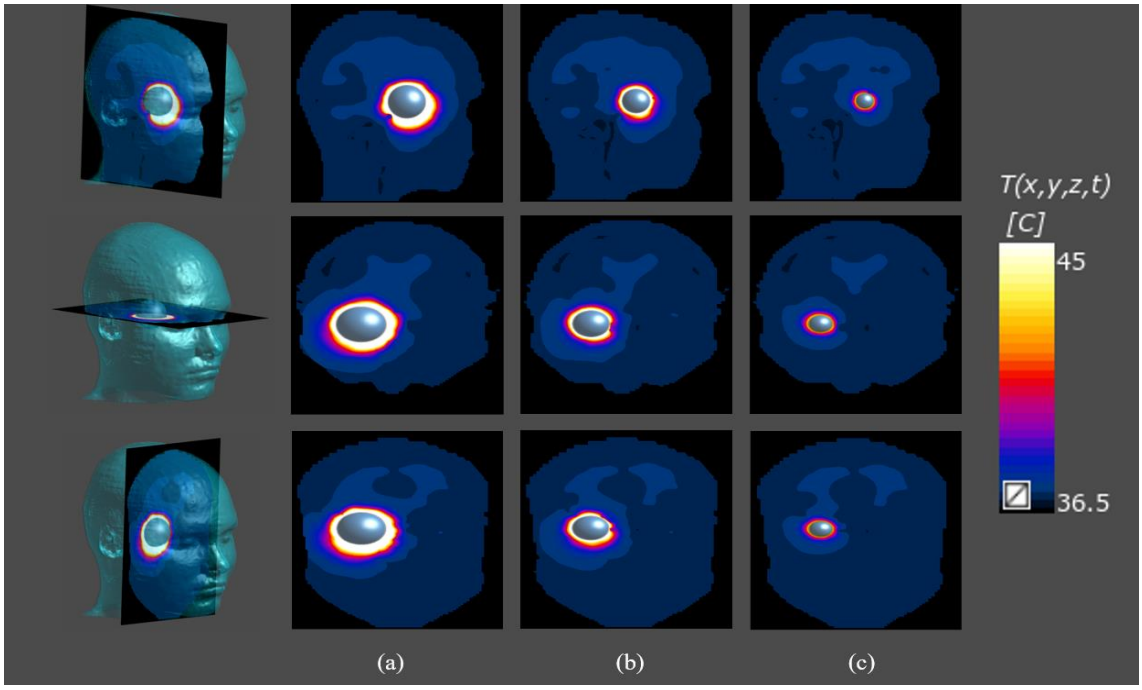

Figure 1: Temperature layout around the 1-coat TBT balloons with a 4 (a), 3 (b) and 2 (c) - cm diameter located in a temporal lobe of MIDA model displayed in sagittal, horizontal and coronal slice, 1800 s after the start of simulation

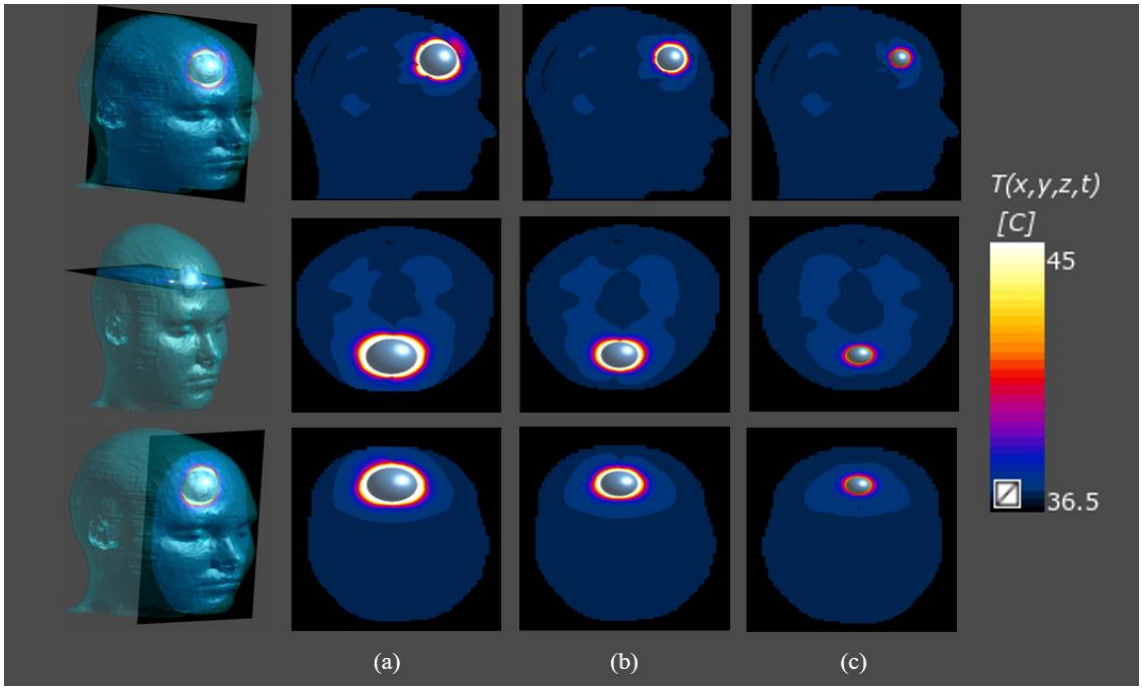

Figure 2: Temperature layout around the 1-coat TBT balloons with a 4 (a), 3 (b) and 2 (c) - cm diameter located in a frontal lobe of MIDA model displayed in sagittal, horizontal and coronal slice, 1800 s after the start of simulation

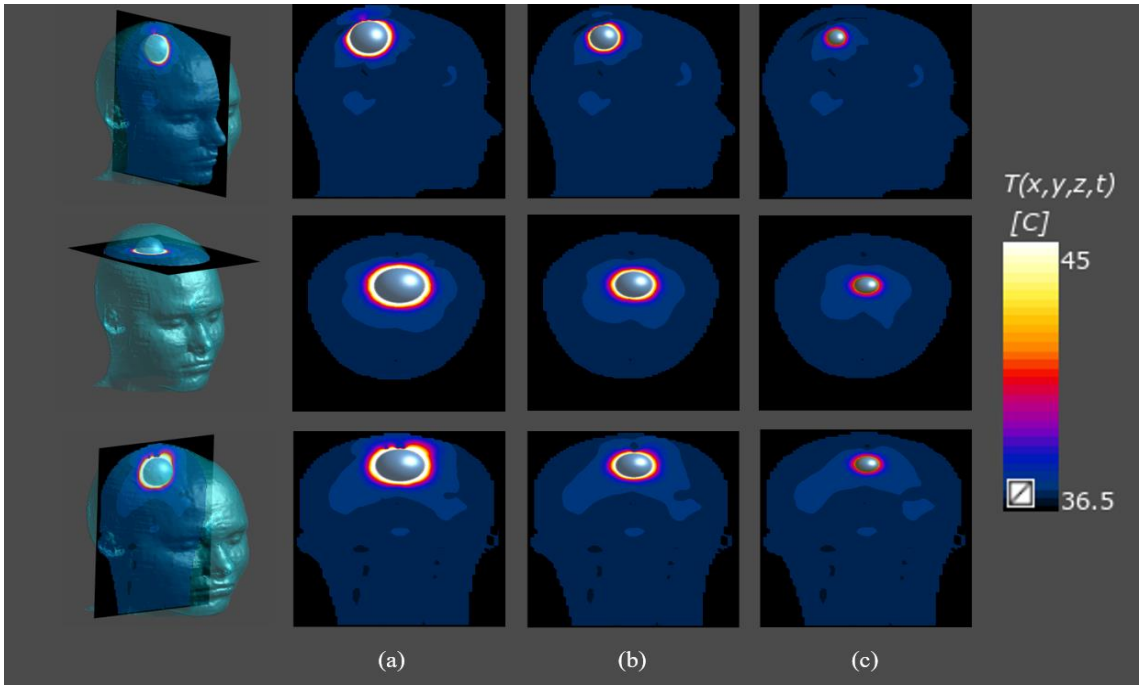

Figure 3: Temperature layout around the 1-coat TBT balloons with a 4 (a), 3 (b) and 2 (c) - cm diameter located in a parietal lobe of MIDA model displayed in sagittal, horizontal and coronal slice, 1800 s after the start of simulation

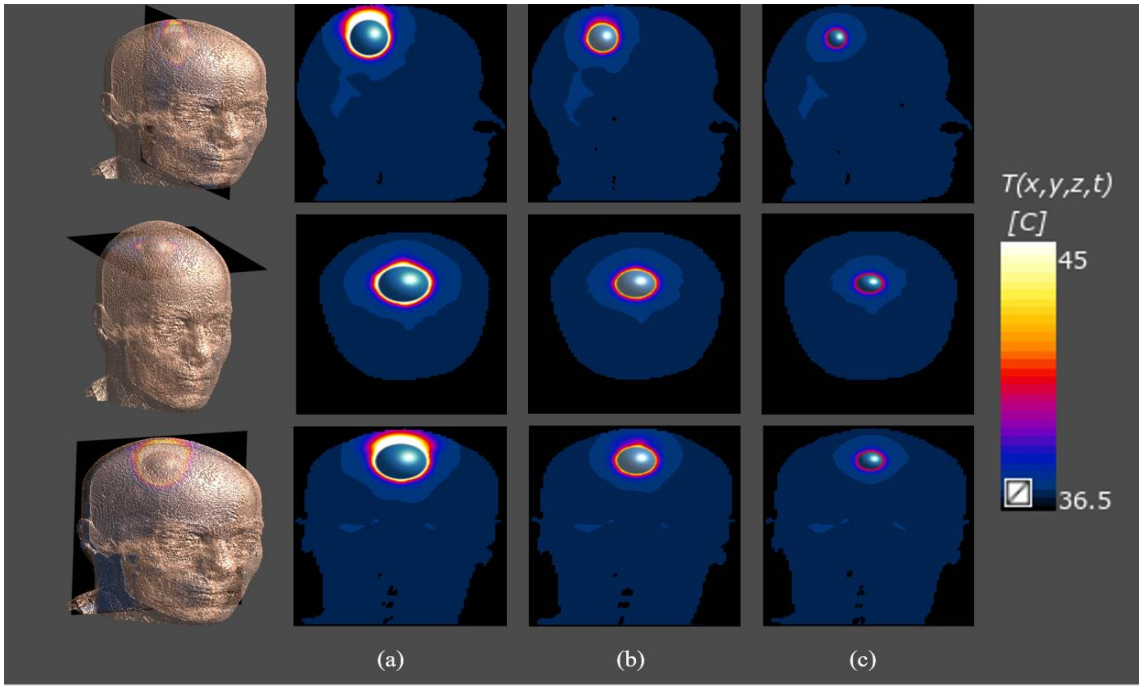

Figure 4: Temperature layout around the 1-coat TBT balloons with a 4 (a), 3 (b) and 2 (c) - cm diameter located in a parietal lobe of patient model displayed in sagittal, horizontal and coronal slice, 1800 s after the start of simulation

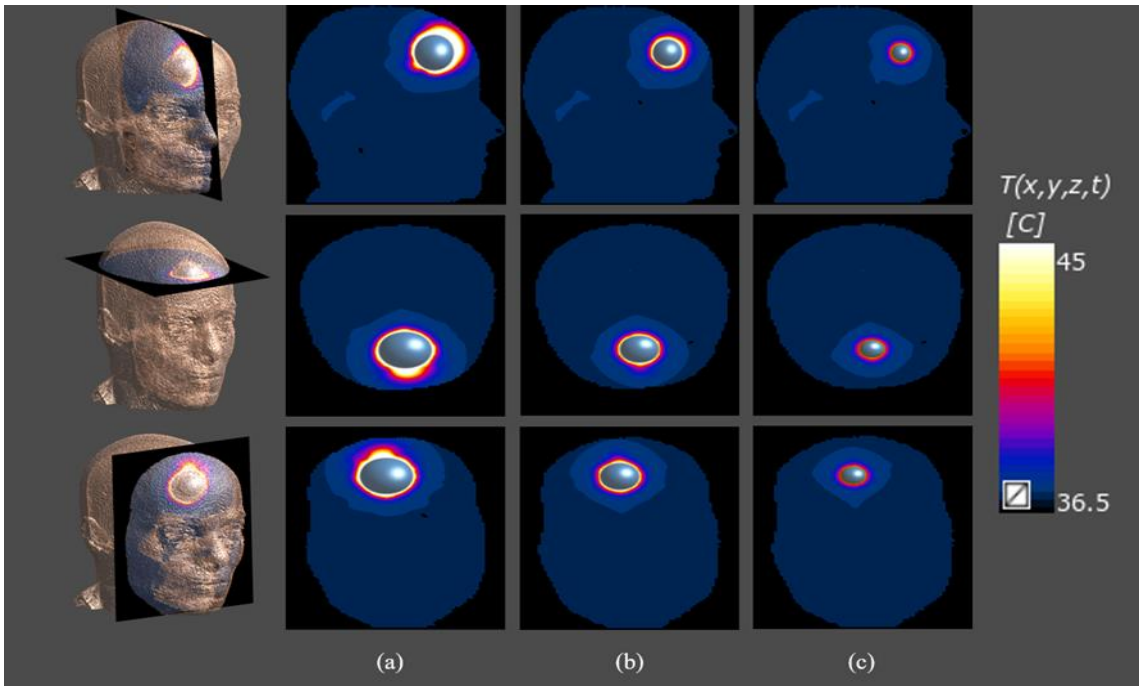

Figure 5: Temperature layout around the 1-coat TBT balloons with a 4 (a), 3 (b) and 2 (c) - cm diameter located in a parietal lobe of patient model displayed in sagittal, horizontal and coronal slice, 1800 s after the start of simulation

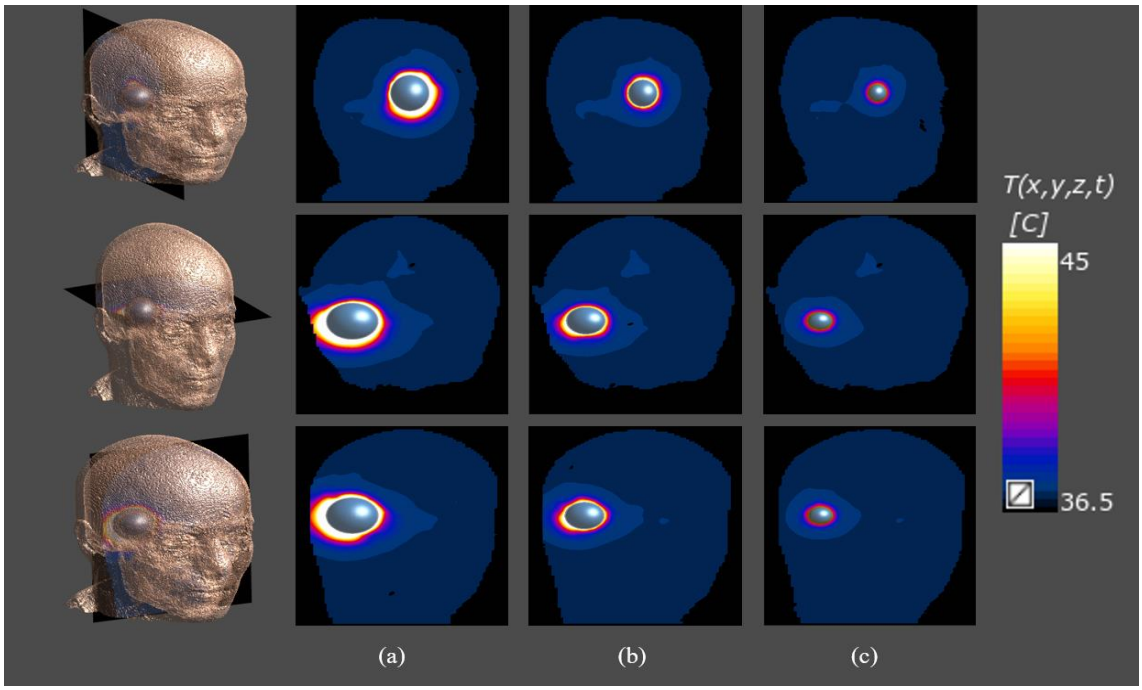

Figure 6: Temperature layout around the 1-coat TBT balloons with a 4 (a), 3 (b) and 2 (c) - cm diameter located in a temporal lobe of patient model displayed in sagittal, horizontal and coronal slice, 1800 s after the start of simulation

Attachment B: Graphs

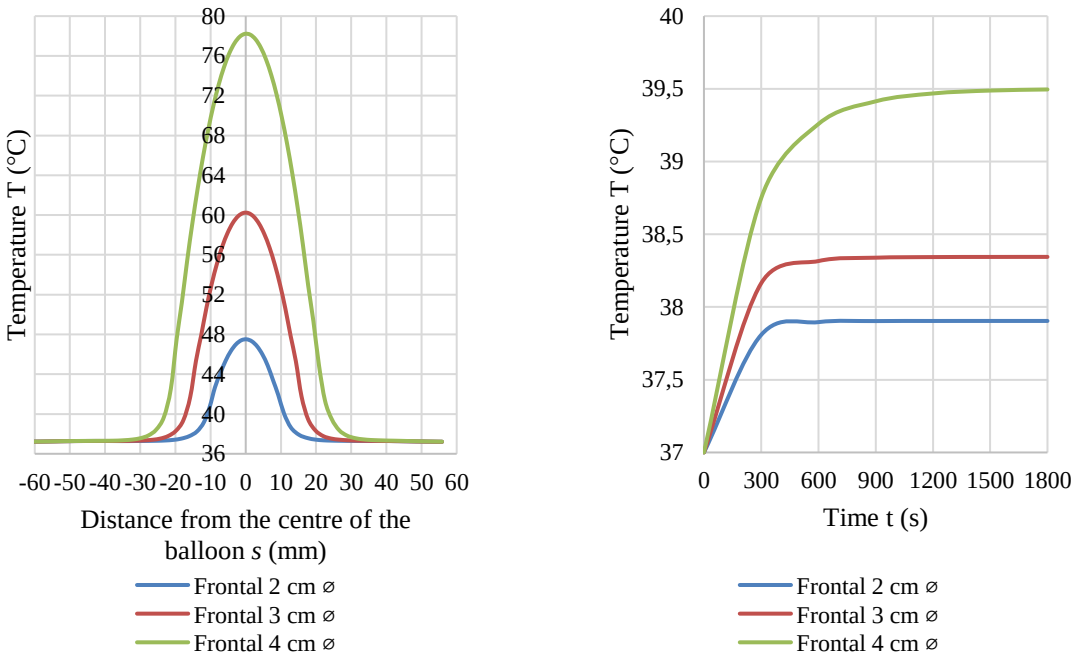

Graph 1: Graphical representation of temperature distribution in the 1-coat TBT balloons and in its vicinity (*left*) and the temperature progression throughout the simulation 5 mm from the balloons (*right*) located in frontal lobe of patient model

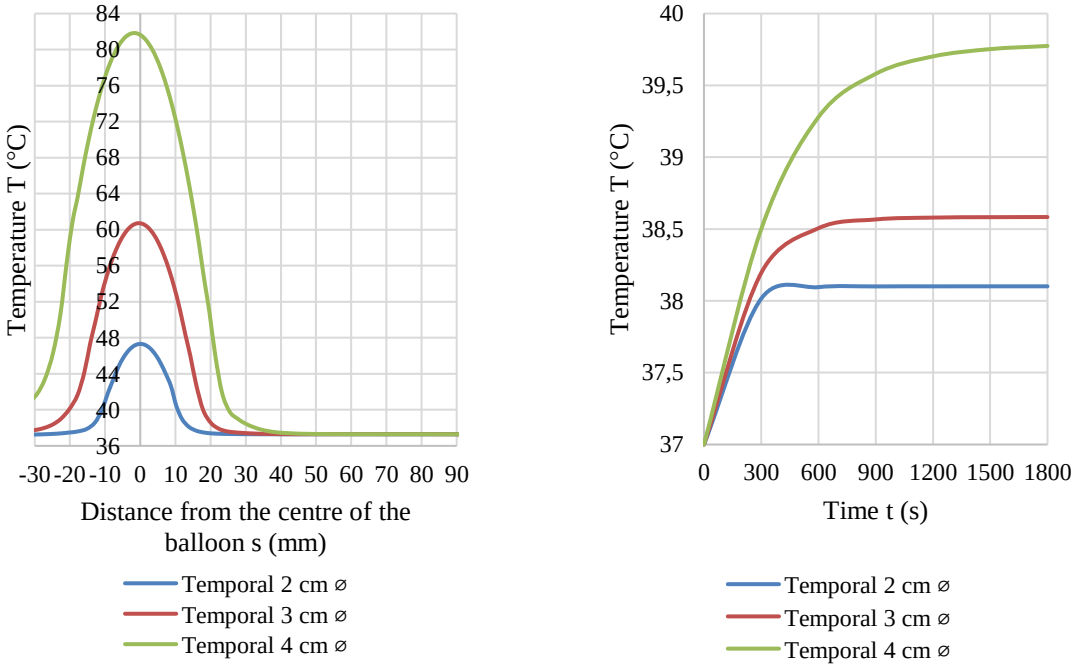

Graph 2: Graphical representation of temperature distribution in the 1-coat TBT balloons and in its vicinity (*left*) and the temperature progression throughout the simulation 5 mm from the balloons (*right*) located in temporal lobe of patient model

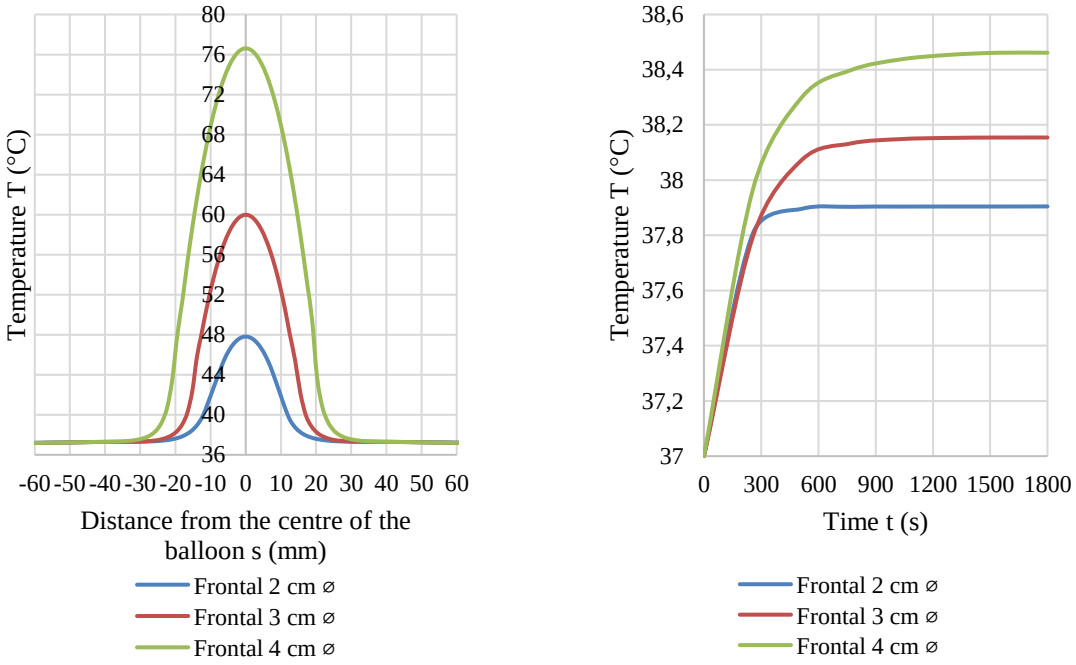

Graph 3: Graphical representation of temperature distribution in the 1-coat TBT balloons and in its vicinity (*left*) and the temperature progression throughout the simulation 5 mm from the balloons (*right*) located in frontal lobe of MIDA model

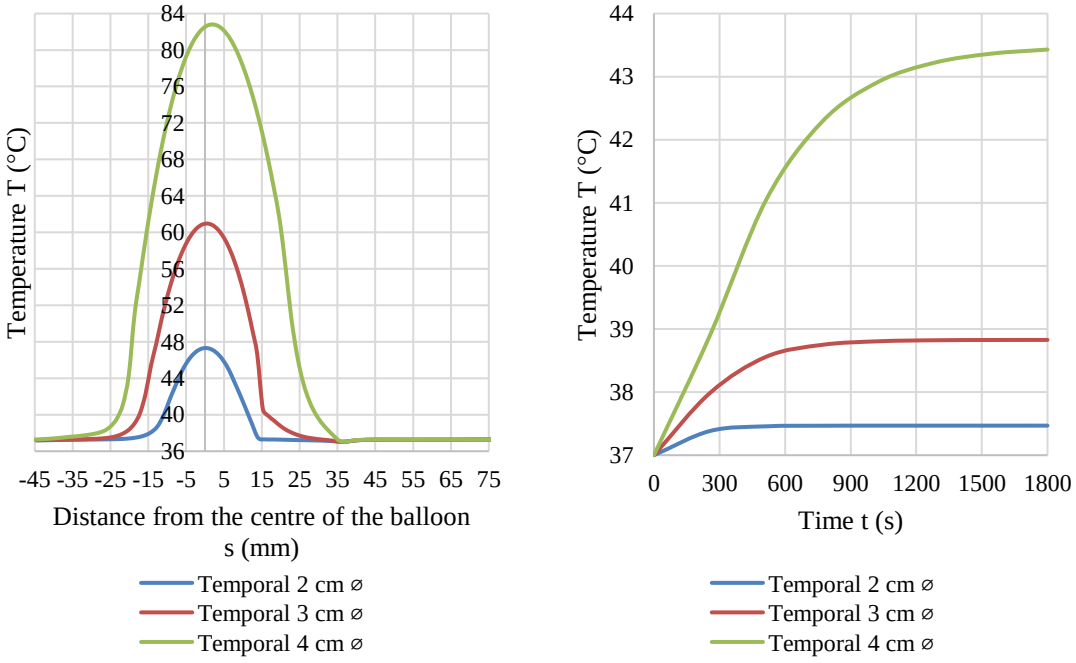

Graph 4: Graphical representation of temperature distribution in the 1-coat TBT balloons and in its vicinity (*left*) and the temperature progression throughout the simulation 5 mm from the balloons (*right*) located in temporal lobe of MIDA model

Attachment C: Content of the enclosed DVD

- Key words (in English and Czech)
- Abstract in English
- Abstract in Czech
- Bachelor Thesis Assignment (in English and Czech)
- Complete Bachelor Thesis
- Simulations in Sim4Life
    - 2-coat models
    - 1-coat models